Design of a Radioisotope Heat Exchanger Rocket

Thomas E. O'Brien*
Montana State University, Bozeman, Montana, 59717

Miles J. McKaig†
University of Illinois, Champaign, Illinois, 61820

Geoffrey A. Landis‡
NASA Glenn Research Center, Cleveland, OH, 44135

The state of planetary exploration vehicle technology has become increasingly more advanced over its long history. Better technologies enable more detailed scientific research to be conducted during the vehicle's life, while advanced manufacturing strategies allow the vehicles to operate for greater lengths of time. However, one aspect of these vehicles has remained constant: the means of exploration. Previous vehicles have all relied on wheels to traverse the surface of the explored planet, limiting their range. The Mars Opportunity Rover, the longest operating rover, only traveled 45.15 km over its life. The radioisotope heat exchanger rocket is a new vehicle concept, designed to use heated gas as a means of propellant. The vehicle collects gas from the surface of a body, stores it in a heated tank, and passes it through a heat exchanger. This process significantly increases the temperature of the collected gas, allowing it to exit through a nozzle with high velocity and efficiency. This process will enable the vehicle to hop across the surface of the body and repeatedly refuel, with the potential of travelling thousands of kilometers during its lifetime. A computer model was constructed to simulate the heat exchanger and nozzle of this proposed system. This simulation allowed the heat exchanger and propellant tank properties to be optimized for the current mission parameters: the exploration of Triton. The nitrogen flows through a 25 kg lithium heat exchanger, consisting of 540, 1.5-mm diameter, 40-cm long Titanium Zirconium Molybdenum pipes, to three operating nozzles. Once landed, the vehicle will conduct science and refueling operations for six days before hopping again. With the optimized design determined from the simulations conducted in this paper, 235.26 kg of nitrogen is collected and stored in a 300 K, 3000 psia tank. With these parameters, a potential hop distance of 39 km with an average specific impulse of 127.5 s is attained. A previous iteration of this vehicle did not include a heat exchanger, instead heating 100 kg of nitrogen to 300 K, only allowing the vehicle to hop 5 km and with a low specific impulse of 60 s. Thus, the addition of the heat exchanger component of the vehicle is shown to potentially double the specific impulse and quadruple the hop distance compared to the previous design.

I. Nomenclature

γ	=	specific heat ratio
η	=	efficiency
ρ	=	density
σ_y	=	yield stress
A	=	cross sectional area
A_s	=	surface area of heat exchanger pipes
C_p	=	specific heat
COPV	=	Composite Overwrapped Pressure Vessel

*NASA Summer Intern, LEX0, Glenn Research Center, Montana State University

†NASA Summer Intern, LEX0, Glenn Research Center, University of Illinois at Urbana-Champaign

‡Researcher, Photovoltaic and Electrochemical Systems Branch, NASA Glenn Research Center, mailstop 302-1, 21000 Brookpark Road, Cleveland OH. AIAA Associate Fellow.

d = distance
D = diameter
f = Darcy friction factor
g_0 = gravitational acceleration on Earth
g_T = gravitational acceleration on Triton
GFSSP = Generalized Fluid System Simulation Program
GPHS = General-Purpose Heat Source
h = convective heat transfer coefficient
I = total impulse
I_{sp} = specific impulse
k = thermal conductivity
l = length
m = mass
$\dot{m}$ = mass flow rate
MW = molecular weight
MLI = Multi-Layer Insulation
NTU = Number of Transfer Units
Nu = Nusselt number
Ov = COPV overwrap percentage
Pr = Prandtl Number
P = pressure
$\mathcal{R}$ = ideal gas constant
R = specific gas constant
r = radius
Re = Reynolds number
RHU = Radioisotope Heating Unit
T = temperature
th = thickness
TZM = Titanium Zirconium Molybdenum
V = volume
u = velocity

Subscripts

avg = average
c = conditions in nozzle chamber
$case$ = lithium block casing
dry = unfueled vehicle
i = conditions in nozzle injector
e = conditions at nozzle exit
p = conditions in heat exchanger pipes
t = conditions at nozzle throat
$tank$ = tank
0 = stagnation
Li = Lithium
N_2 = Nitrogen
$shell$ = tank shell
sys = lithium block system
$tubes$ = heat exchanger tubes

II. Introduction

TRITON is a large, icy moon of the planet Neptune. It is 1682 km in diameter, with a surface gravity of 0.779 m/s^2 (0.0794g) and a cryogenic surface temperature of 34 K. Its surface is mostly comprised of nitrogen ice and it has a

thin atmosphere, also composed mainly of nitrogen, with small amounts of methane. It is a fairly unusual moon, for it orbits Neptune in a retrograde motion. Additionally, its surface has large quantities of tholins, a variety of organic compounds thought to potentially be the precursors to life. Tholins are common throughout the outer solar system. For these reasons, Triton is thought to be a captured Kuiper belt object, with an origin and composition similar to Pluto. With active nitrogen geysers and surface features ranging from cantaloupe style terrain to mountain ranges, Triton is one of the only moons within our solar system to be geologically active. Despite these notable characteristics, Triton has only been visited once, by Voyager 2 in 1989. This icy moon is therefore an ideal place to explore and learn about the origins of life and the solar system.

The radioisotope heat exchanger rocket, for this mission dubbed the 'Triton Hopper', is an exploration vehicle capable of in-situ resource utilization. On a celestial body like Triton, this means that the rocket can utilize the nitrogen ice on the surface or the nitrogen contained within the atmosphere as a propellant. The rocket also contains a radioisotope heat source — Four General-Purpose Heat Source blocks (GPHS), located within the heat exchanger assembly, which provide a total of 1kW thermal power at a temperature of 1200 °C. A portion of the heat output from these blocks is converted to electrical power by Stirling engines . The rejected waste heat from these engines is used to heat the propellant tank to the storage temperature of 300 K. The remaining thermal energy from the GPHS source is directed to raising the temperature of a thermal block, storing the heat energy in a mass of lithium to an equilibrium temperature of 1200 °C. The heat exchanger itself is composed of 25 kg of lithium with 540 pipes, each 1.5 mm in diameter and 40 cm long, passing through.

Once landed on the surface, the vehicle will conduct various scientific operations. Meanwhile, the rocket will also begin harvesting the nitrogen propellant. The rocket is designed to carry approximately 235 kg of nitrogen propellant, stored at 300 K and 3000 psi. After the propellant is collected and scientific operations are complete, the rocket will hop across the surface to a new location. The nitrogen stored in the tank is passed through the heat exchanger, raising its temperature to values as high as 1200 K. The gas then flows through three operating nozzles, providing thrust.

This concept provides many design challenges. A system like this is highly coupled, making it difficult to optimize. Various computer software programs were utilized to best model the system and its components to aid in the optimization process. Optimization parameters include propellant tank pressure, propellant temperature, as well as the ratio between the amount of nitrogen propellant and lithium mass. All these parameters have an impact on the performance of the rocket. These simulations allowed the rocket to be optimized for the maximum possible hop distance.

III. Heat Exchanger Model

The core component of this rocket concept is the thermal storage medium and the heat exchanger itself. Various studies were performed to best characterize the system. Essentially, the thermal storage medium is composed of heated material which fluid flow pipes pass through, allowing heat transfer to occur. As the propellant flows through the heat exchanger, heat is drawn out of the material and into the fluid. Since the heat storage is of a finite mass, only a finite amount of heat energy can be stored. This makes the material used for thermal energy storage critical to the performance of the system and can best be described as a thermal battery. Materials that perform best for this application will have high values of density, specific heat (C_p), and thermal conductivity.

A. Previous Analysis

Initial studies of potential thermal energy storage media looked at materials including those with a phase-change region within the operating temperature range. These materials included lithium, lithium fluoride, beryllium, copper, and aluminum [1]. Phase-change regions increase performance by drawing out a constant amount of energy (the latent heat of fusion) while the material, now considered a *phase-change material*, changes from a liquid to a solid. Of the materials listed above, only lithium, lithium fluoride, and aluminum include a phase-change region for the conditions of this system. Figure 1 shows the amount of heat energy released by the materials studied within a temperature range of 900 to 0 °C. Note the vertical discontinuities of the plots. These represent the phase-change region of the materials. Based on the temperature range experienced in the system, lithium was chosen to be the most ideal material.

The previous study also performed various heat transfer calculations. One such calculation was composed of a system of 1000 pipes of 1 mm diameter and 20 cm in length, with 35 kg of nitrogen propellant. The initial temperature of the nitrogen was assumed to be −100 °C and the pipe wall temperature was assumed to be a constant 900 °C, with a total mass flow rate of 0.1 kg/s. With 1000 tubes, the mass flow rate per tube is 1.0×10^{-4} kg/s. Given this information, the fluid exit temperature was calculated.

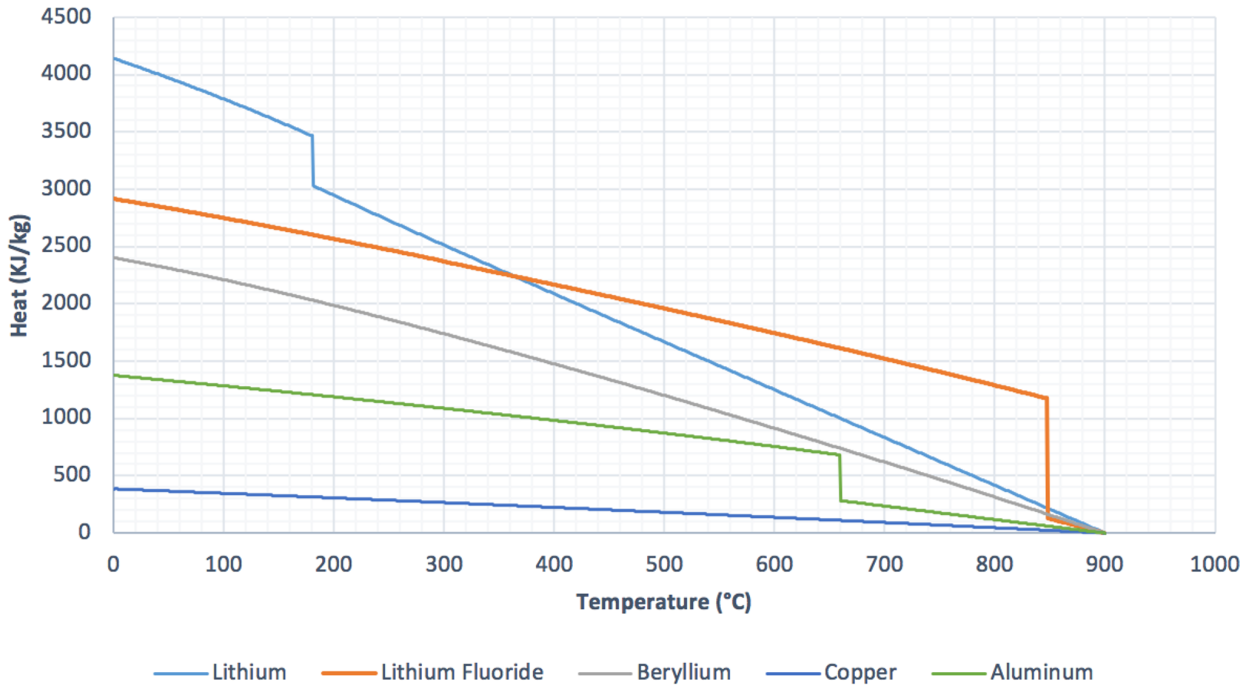

Fig. 1 Heat Released vs. Temperature

Based on the ideal gas law, the nitrogen density can be calculated.

$$V = \frac{nRT}{P} = \left(\frac{35\,\text{kg}}{0.028\,\frac{\text{kg}}{\text{mol}}}\right) = 0.261\,\text{m}^3 \tag{1}$$

$$\rho = \frac{m}{V} = 134.4\frac{\text{kg}}{\text{m}^3} \tag{2}$$

The average velocity of the fluid in the pipe can then be calculated.

$$A_p = \frac{\pi}{4}D_p^2 = \frac{\pi}{4}(0.001\,\text{m})^2 = 7.85\times10^{-7}\text{m}^2 \tag{3}$$

$$u_{avg} = \frac{\dot{m}}{\rho A_c} = \frac{0.0001\,\frac{\text{kg}}{s}}{134.3\,\frac{\text{kg}}{\text{m}^3}\,(7.85\times10^{-7}\text{m}^2)} = 0.95\frac{\text{m}}{\text{s}} \tag{4}$$

The Reynolds number can be calculated.

$$Re = \frac{\rho u_{avg} D_p}{\mu} = \frac{(134.3\,\frac{\text{kg}}{m^3})(0.95\,\frac{\text{m}}{\text{s}})(0.001\,\text{m})}{2.267\times10^{-}5} = 5615.67 \tag{5}$$

As the Reynolds number is greater than 4000, the flow is turbulent, so the Prandtl and Nusselt numbers, and the convective heat transfer coefficient, can be calculated as shown below to solve for the tube exit temperature.

$$Pr = \frac{\mu C_p}{k} = \frac{\left(2.267\times10^{-5}\,\frac{\text{kg}}{\text{ms}}\right)\left(1.0458\,\frac{\text{kJ}}{\text{kgK}}\right)}{0.0339\,\frac{\text{W}}{\text{kgK}}} = 0.70 \tag{6}$$

$$Nu = \frac{(f/8)(Re-1000)Pr}{1+12.7(f/8)^{1/2}\left(Pr^{2/3}-1\right)} = \frac{0.70(0.037/8)(5615.67-1000)}{1+12.7(0.037/8)^{1/2}\left(0.70^{2/3}-1\right)} = 18.42 \tag{7}$$

$$Nu = \frac{hD}{k} \rightarrow h = \frac{Nu\,k}{D} = \frac{18.42\,(0.0339\,\frac{\text{W}}{\text{mK}})}{0.001\,\text{m}} = 625\,\frac{\text{W}}{\text{m}^2\text{K}} \tag{8}$$

The number of transfer units can be calculated as,

$$A_s = \pi DL = \pi(0.001\,\text{m})(0.2\,\text{m}) = 0.000\,628\,3\,\text{m}^2 \tag{9}$$

$$NTU = \frac{hA_s}{\dot{m}C_p} = \frac{\left(625\ \frac{\text{W}}{\text{m}^2\text{K}}\right)(0.000\,628\,3\,\text{m}^2)}{0.0001\ \frac{\text{kg}}{\text{s}}\left(1.0458\ \frac{\text{kJ}}{\text{kgK}}\right)} = 3.75 \tag{10}$$

With an NTU value close to 5, the temperature at the exit of the tubes is close to the surface temperature of the tubes, and the value can be used to yield the actual temperature of,

$$T_c = T_s - (T_s - T_i)\exp\left(-\frac{hA_s}{\dot{m}C_p}\right) = 900\,^\circ\text{C} - (900\,^\circ\text{C} + 100\,^\circ\text{C})\exp(-3.75) \tag{11}$$

$$T_c = 877\,^\circ\text{C} \tag{12}$$

As estimated from this simplified analysis, the nitrogen propellant can be heated to values close to the initial temperature of the heat exchanger. However, this analysis fails to incorporate several important aspects of the system. For the nitrogen, the temperature entering the heat exchanger is constantly changing as the pressure in the tank decreases. This changes the inlet density to the heat exchanger as well. Furthermore, as the temperature of the nitrogen increases as it flows through the heat exchanger, its density and velocity continue to change. A constant surface temperature for the pipe walls also cannot be assumed, as the whole principle of the heat exchanger is to draw heat out of the lithium, thereby decreasing the temperature. For these reasons, a more robust model of the system was required to accurately depict the properties of the propellant and the state of the heat exchanger.

B. GFSSP Model

GFSSP, Generalized Fluid System Simulation Program, is a computer modeling simulation developed at NASA Marshall Space Flight Center to analyze fluid flow parameters. The program uses a finite volume method to simulate flow in a network of nodes and branches, and calculates properties throughout the system. In addition to simulating the flow of nitrogen in the system, GFSSP can model conjugate heat transfer in the system, incorporating the flow of heat from the solid thermal block to the nitrogen, and the resulting effects on the nitrogen flow. As a numerical model with time- and position-dependent flow and heat transfer properties, it is expected to be more accurate than the initial analytical approximation.

The model developed for the system, shown in Figure 2, models the system as a set of parallel pipes, surrounded by a mass of lithium. To improve accuracy and provide more detailed information, the block is split into 10 length segments, and 11 sets of fluid nodes, measuring nitrogen pressure and temperature throughout the block's length, modeling the flow as a transient system. The nitrogen is supplied by a finite volume tank, such that the simulation includes the effects of tank blowdown and Joule-Thomson cooling on the inlet temperature of nitrogen to the heat exchanger. Heat transfers from the lithium to the nitrogen by convection, and between sections of the lithium block by conduction.

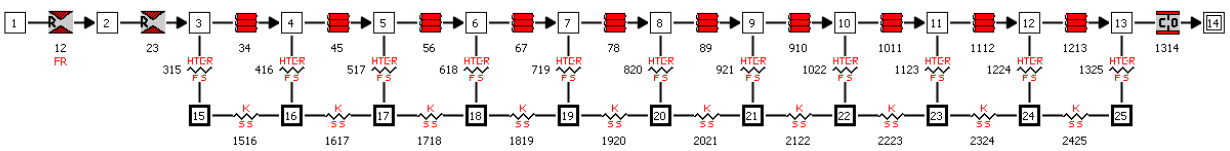

Fig. 2 GFSSP Model Diagram

Since the lithium temperature decreases over time, the exit temperature is best compared at the initial peak condition of flow. The GFSSP model was fed the conditions of the previous study and run for 2 seconds. The final conditions were then used to avoid anomalous data from initial peaks due to flow startup in the transient model. These results are tabulated in Table 1. The exit temperature is much lower than expected. This result is believed to be due to the compressible nature of the flow. The GFSSP model simulates a changing density system and tops out at Mach 0.84 in the exchanger tubes, indicative of Rayleigh flow heating. By comparison, the previous study assumed a constant density, and does not incorporate the effects of Rayleigh flow, and as such does not have a maximum enthalpy condition.

Table 1 Comparison of calculated gas exit temperature T_c from the GFSSP model with the analytical model

Initial Li Temperature [K]	Tube Diameter [mm]	Tube Length [cm]	Flow Rate [kg/s]	Analytic T_c [K]	GFSSP T_c [K]	Difference [%]
1173.15	1	20	0.1	1150	983.55	16.9

Even considering these differences, the error is quite small at 16.9%, with the results of the GFSSP model being limited by Rayleigh flow choking. As such, the GFSSP model was considered to be a more accurate representation of the system.

C. ANSYS® Model

ANSYS® is another computer simulation program used to analyze various engineering problems. It uses a finite element model and can be used to analyze various systems, such as structural, thermal, and fluid flow models. For the purposes of this analysis, it was used to confirm the GFSSP flow results and view the system in three dimensions. It also can provide data that GFSSP cannot, including: solid/liquid ratio, 3D temperature and velocity gradients, and convective current diagrams. However, it also requires much more computing power. For this reason, only a small section of the heat exchanger was modeled, as shown in Figure 3. Even with a subsection this small, the mesh contains several million elements, making the simulation extremely slow to run with the computational resources available. The ANSYS simulation was modeled for the settings provided in Table 2.

Table 2 ANSYS Model Initial Conditions

Li Mass [kg]	Li Temperature [K]	Tank Pressure [psia]	Tank Temperature [K]	Tank Volume [m^3]	Total N_2 Mass [kg]	Flow Rate [kg/s]
25	1373.15	1000	300	1.7	132	0.9

The simulation was run for 84.5s of system flow time, with a variable time step of at most 0.1 seconds to maintain convergence, and data shown for 22.8 seconds and 84.5 seconds. Execution required around 24 hours of computational time, far exceeding the GFSSP computational time, limiting the usefulness of the model. Nonetheless, it provided valuable insight into the verification of the GFSSP model.

The ANSYS results for 22.8 seconds can be seen below in Figures 4, 5, and 6. Figure 4 shows the temperature distribution within the lithium block. The maximum temperature of 1322 K occurs at the outlet end of the block while the minimum temperature occurs at the nitrogen inlet. Figure 5 provides the velocity gradient through the nitrogen flow. The flow accelerates from very low inlet speeds to a peak velocity of 735 m/s near the outlet. However, the average speed in the region is approximately 706 m/s, or about Mach 1.122. This indicates the ANSYS results may not be

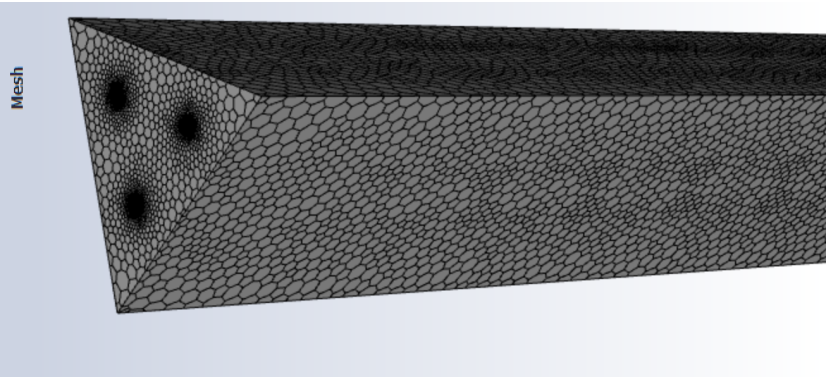

Fig. 3 Finite-element mesh of three heat-exchanger tubes embedded in the lithium thermal block, as used in the ANSYS simulation.

properly accounting for the transonic flow region, or potentially pointing to an additional phenomenon due to the exit conditions in the model. Figure 6 shows the temperature gradient of the nitrogen at the outlet. The nitrogen flowing along the wall is very close to the wall temperature, at 1300 K, with lower temperatures in the center flow for an average exit temperature of 994 K.

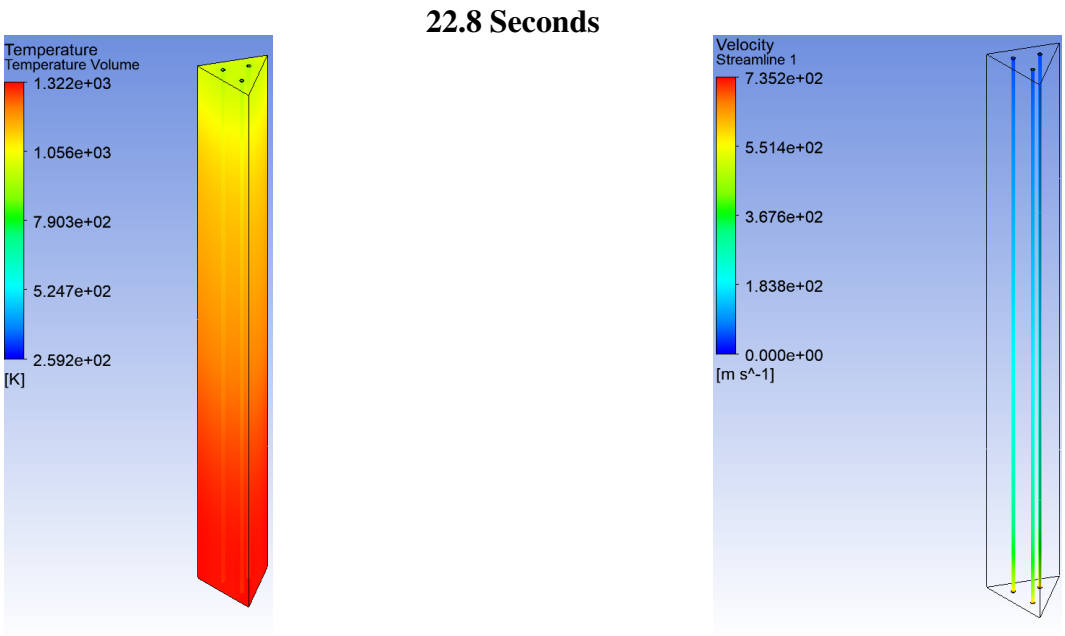

Fig. 4 Lithium Temperature Gradient

Fig. 5 N_2 Velocity Gradient

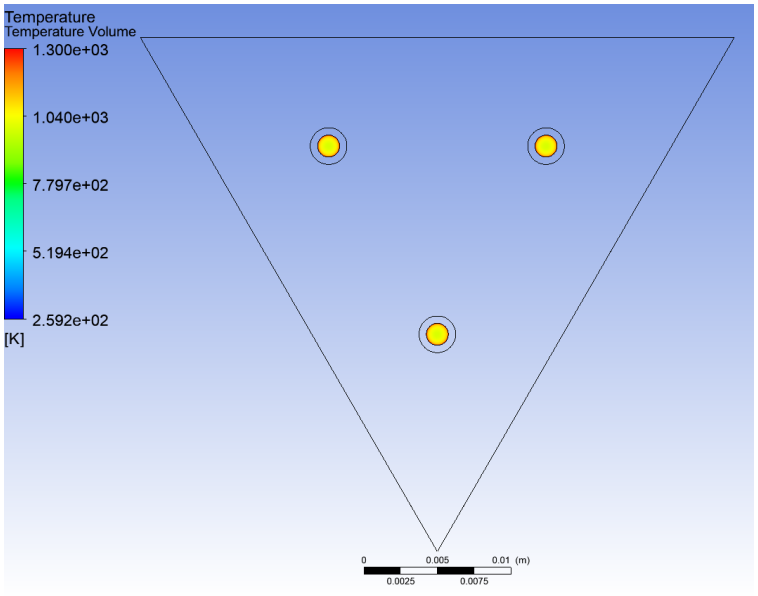

Fig. 6 N_2 Outlet, T_{avg} = 994 K

The results for the same system at 22.8 seconds run through GFSSP are shown in Figures 7 and 8 below. Figure 7 is a profile view of the fluid temperature in the system at 22.8 seconds. The inlet temperature is on the left, and the outlet is the peak temperature of 985 K on the right. The final drop in temperature is due to the reduction to the fixed ambient conditions of Triton outside the nozzle, and without backflow has no effect on the upstream conditions. Figure 8 shows a profile view of the lithium temperature at 22.8 seconds, again with inlet side on the left, with a temperature of 1163.15 K, and outlet side at 1283.15 K on the right.

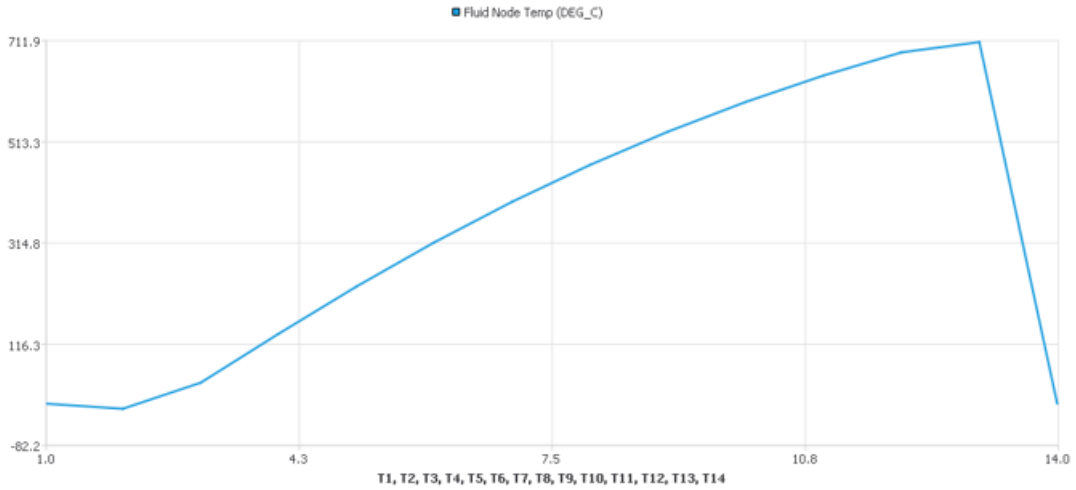

Fig. 7 N_2 Temp Through Heat Exchanger, T_{Out} = 985 K

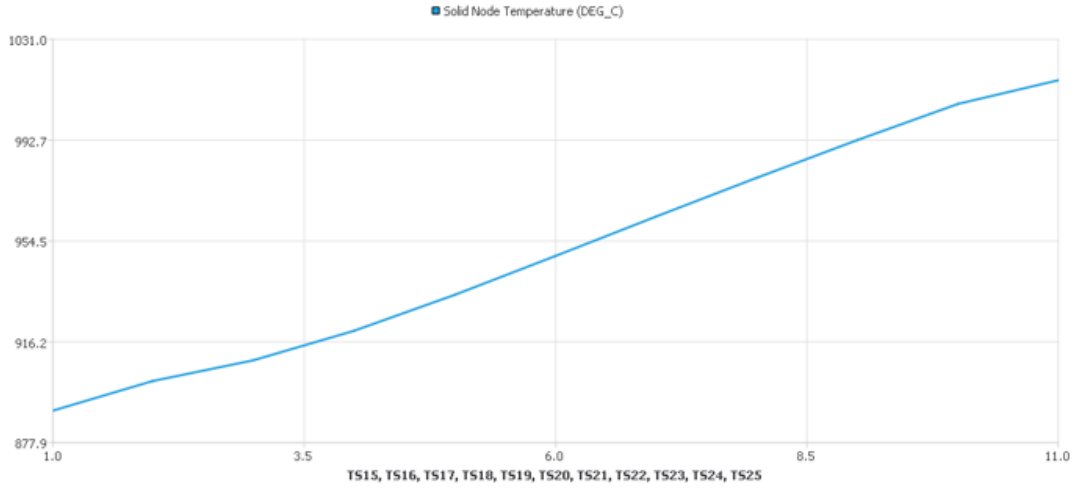

Fig. 8 Lithium Temperature, T_{In} = 1163.15 K, T_{Exit} = 1283.15 K

The results from ANSYS for 84.5 seconds can be seen below in Figures 9, 10, and 11. Figure 9 shows the temperature distribution within the lithium block. The temperature throughout the block has reduced significantly. The maximum temperature of 813.6 K occurs at the outlet end of the block while the minimum temperature occurs at the nitrogen inlet, much like the results for 22.8 seconds. Figure 10 provides the velocity gradient through the nitrogen flow. The flow accelerates from low inlet speeds to a peak velocity of 514 m/s near the outlet, with an average speed of approximately 492 m/s, or about Mach 1.04, similarly indicating a modeling inaccuracy. Figure 11 shows the temperature gradient of

the nitrogen at the outlet. The boundary layer flow is still very close to the wall temperature, at 795 K, and the center flow is significantly colder, for an average exit temperature of 541 K.

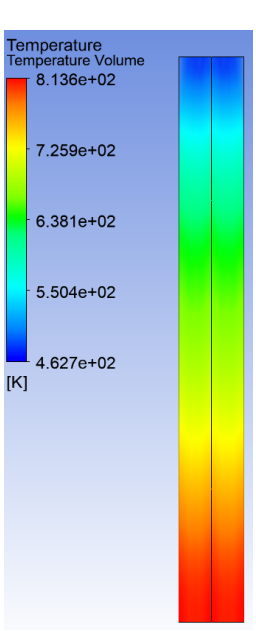

Fig. 9 Lithium Temperature Gradient

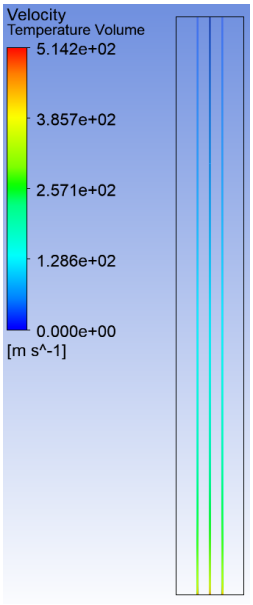

Fig. 10 N_2 Velocity Gradient

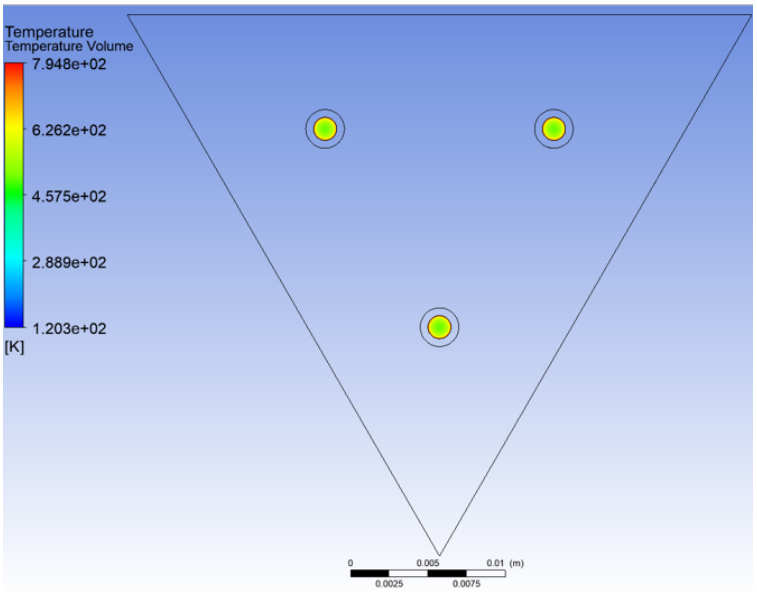

Fig. 11 N_2 Outlet, T_{avg} = 541 K

The results for the same system at 84.5s run through GFSSP are shown in Figures 12 and 13 below. Figure 12 provides the fluid temperature profile of the model at 84.5 seconds, with inlet conditions on the left, and the peak temperature of 730.15 K at the exit on the right, and a final drop once again to the fixed Triton ambient conditions. Figure 13 shows the lithium temperature temperature profile at 84.5 seconds, with the inlet side temperature of 769.15 K on the left, and the exit side temperature of 1045.15 K on the right end.

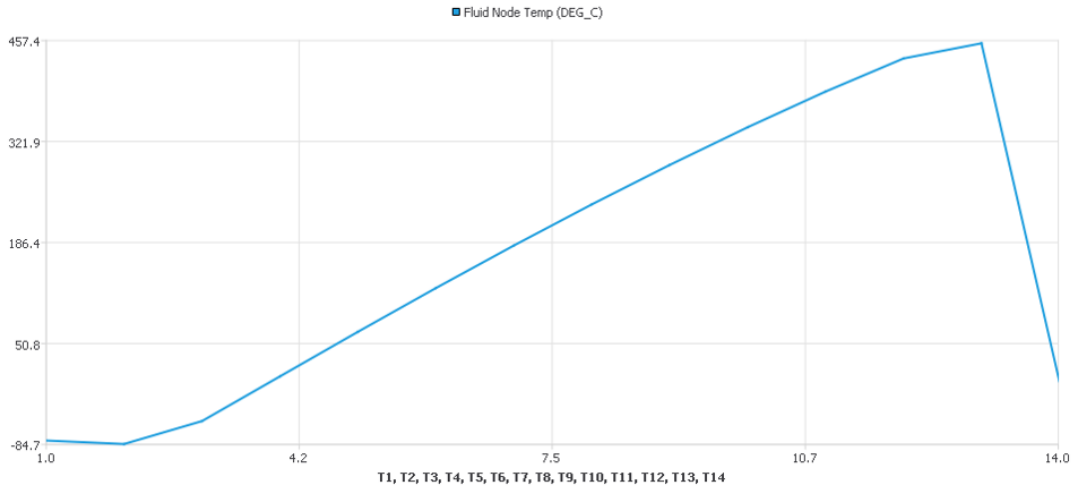

Fig. 12 N_2 Temp Through Heat Exchanger, T_{Out} = 730.15 K

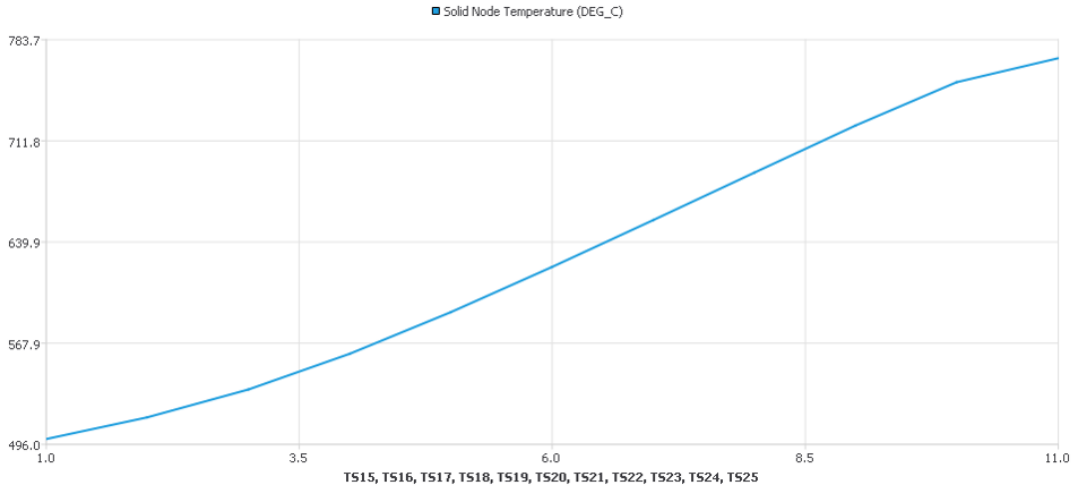

Fig. 13 Lithium Temperature, T_{In} = 769.15 K, T_{Exit} = 1045.15 K

The model error comparisons are shown in Table 3. At the 22.8 second time step, the predicted temperatures for the exit conditions of the nitrogen are shown to have very little divergence between the two models. The inlet side of the lithium has a larger 20% error, however the outlet side has a much smaller error of only 1%. At the 84.5s time step, the models have significantly diverged. This could be due to differences between the modeling software, particularly initialization conditions or transonic model behavior. Small time steps, therefore, can be considered accurate.

While ANSYS provides detailed analysis, the complexity of the initialization and other parameters, as well as the considerably lengthy computational times, led to the decision of using GFSSP as the primary system model.

Table 3 Error Calculations

Variable	Time Step [s]	ANSYS Result [K]	GFSSP Result [K]	Error [%]
T_{out}	22.8	994	980.55	1.35
	84.5	541	725.3	34.06
$T_{Li,in}$	22.8	969	1163.88	20.11
	84.5	469.541	771.95	64.40
$T_{Li,out}$	22.8	1302.27	1288.1	1.09
	84.5	799.445	1042.65	30.42

IV. Engine Optimization

As with any spacecraft, optimization is a critical component to designing a successful and efficient vehicle. This system has many coupled variables that affect its performance. Tank pressure, tank temperature, tube length, tube diameter, lithium mass, and lithium temperature are all variables that have an impact on each other and the system as a whole. Once GFSSP was confirmed to be an accurate and efficient model for this system, a parametric analysis on these variables was initiated. The goal of the optimization was to maximize the total hop distance. Each individual variable and combinations thereof were analyzed to determine their impact on the system.

A. Initial Optimization

Each individual variable was analyzed for its effect on the final N_2 temperature and final solid temperature. The changes with a positive influence were coupled together to attempt to maximize the performance. The results are shown in Table 4, collected from simulations of 50 seconds of flow. Generally, lengthening the heat exchanger pipes and limiting the number of tubes to around 500 had the best performance impact. Raising the solid mass did have diminishing returns, so an initial optimum of 25kg was selected.

Table 4 Results for Varying System Geometries

Case #	Li Mass [kg]	# of Tubes	l_{tubes} [cm]	D_{tubes} [mm]	Peak Temperature [°C]	Minimum Li Temperature [°C]
Control	15	1000	30	2	716.8	608.9
1	22	1000	40	1	974.7	456.4
2	22	500	40	1	951.0	462.5
3	25	500	40	1	951.0	513.2
4	22	500	45	1	981.1	420.0
5	22	500	35	1	912.3	510.3
6	25	500	35	1	912.4	575.1
7	25	500	35	1.5	815.0	694.6
8	25	500	40	1.5	861.3	654.3
9	25	750	40	1.5	880.9	645.5
10	25	500	35	1.25	859.9	651.4
11	25	540	35	1.5	819.0	692.8
12	25	540	40	1.5	865.0	652.6
13	25	630	35	1.5	827.0	689.3
14	25	630	40	1.5	872.5	649.2
15	25	720	35	1.5	833.9	686.3
16	25	720	40	1.5	879.0	646.3

Many of the intial results were analyzed on the assumption that the thermal block was heated by the GPHS to an initial temperature of 900 °C. Since the specific impulse of the engine increases approximately proportional to the square root of the temperature of the gas, in this analysis the thermal block temperature was increased. References show that existing Radioisotope Power Systems using GPHS can operate to temperatures of 1100 °C [2, 3]. The Pu fuel elements themselves have been tested to survive 2360 °C, but an upper limit of 1500 °C is set by the requirement of non-reactivity of the plutonium pellet with the iridium coating. Based on this information, in consultation with the subject matter experts on the GPHS fuel elements, the target thermal block temperature was increased to a baseline initial temperature of 1200 °C (1473 K). The higher thermal leak rate (seen in Figure 19) due to the higher temperature meant that an additional GPHS brick would be required to achieve the higher temperature, but since the mass of the GPHS block itself is small compared to the rest of the system, this was not considered to be a major issue.

B. MATLAB® Optimization

With a better understanding of the effects of various parameters effect on the system, a more complex method of optimization was created. Results from GFSSP can be outputted to comma separated value (CSV) format, allowing external programs to access them. A MATLAB® script was created, as shown in Listing 1 in Appendix B. The script takes the large quantities of data provided from GFSSP, outputted to CSVs, and processes this down into performance data.

The script first calculates the total conditions in the chamber of the nozzle as

$$a_c = \sqrt{\gamma R T_c} \tag{13}$$

$$M_c = \frac{u_c}{a_c} \tag{14}$$

$$T_{0c} = T_c \left(1 + \frac{\gamma - 1}{2} M_c^2\right) \tag{15}$$

$$P_{0c} = P_c \left(1 + \frac{\gamma - 1}{2} M_c^2\right)^{\frac{\gamma}{\gamma - 1}} \tag{16}$$

These total conditions can then be used to find the nozzle exit velocity of the nitrogen

$$u_e = \sqrt{\frac{2\gamma R}{(\gamma - 1)MW} T_{0c} \left(1 - \left(\frac{P_e}{P_{0c}}\right)^{\frac{\gamma - 1}{\gamma}}\right)} \tag{17}$$

Since the atmosphere on Triton is near vacuum, a large nozzle area ratio is ideal, and the desired ratios result in very low ratios of exit pressure to chamber pressure. Therefore, the equation for the exit velocity can be approximated and used to find thrust and specific impulse as

$$u_e = \sqrt{\frac{2\gamma R}{(\gamma - 1)MW} T_{0c}} \tag{18}$$

$$F = \eta \dot{m} u_e \tag{19}$$

$$I_{sp} = \eta \frac{u_e}{g_0} \tag{20}$$

with η as the engine's efficiency.

Using these results, the total impulse of the engine can be calculated until time t_{end},

$$I = \int_0^{t_{end}} F(t) dt \tag{21}$$

This total impulse can also be used to calculate an approximate hop distance of the vehicle,

$$\Delta v = \frac{I}{m_{dry} + m_{N_2,total} - \frac{m_{N_2,used}}{2}} \tag{22}$$

$$d = \frac{\eta_{\Delta v} \Delta v^2}{4 g_T} \tag{23}$$

where $\eta_{\Delta v}$ accounts for additional Δv margin and maneuvering thruster propellant usage during coast.

With a way to estimate the hop distance, optimum configurations were determined by varying different parameters of the system, including initial tank pressure and temperature, and the ratio of nitrogen mass to lithium mass. To do so properly, the variable dry mass of the system needed to be included, in order to identify when the mass of the vehicle reduced the system's overall performance. A set of functions were therefore included to calculate the weight of the tank and of the lithium block assembly.

First, with a total number of tubes, n_{tubes}, inner and outer diameters $D_{i,tubes}$ and $D_{o,tubes}$, respectively, and tube length l_{tubes}, the mass of the heat exchanger tubes is given by:

$$m_{tubes} = \rho_{tubes}\left(\frac{\pi n_{tubes} l_{tubes}}{4}\left(D_{o,tubes}^2 - D_{i,tubes}^2\right)\right) \tag{24}$$

The lithium block is assumed to be cylindrical, with the heat exchanger tubes running through it, and GPHS blocks in the core. The net volume of the lithium, tubes, and GPHS blocks can be found as,

$$V_{Li} = \frac{m_{Li}}{\rho_{Li}} \tag{25}$$

$$V_{tubes} = n_{tubes} l_{tubes} \frac{\pi}{4} D_{o,tubes}^2 \tag{26}$$

$$V_{GPHS} = n_{GPHS}\,(0.1\text{ m} \times 0.1\text{ m} \times 0.05\text{ m}) \tag{27}$$

$$V_{net} = V_{Li} + V_{tubes} + V_{GPHS} \tag{28}$$

With a volume, and a chosen block length, a block radius can then be derived,

$$r_{net} = \sqrt{\frac{V_{net}}{\pi l_{tubes}}} \tag{29}$$

Finally, assuming the casing is an outer cylindrical layer with thickness th_{case}, the casing mass and total system mass can be calculated,

$$m_{case} = \rho_{case}\left(2\pi(r_{net} + th_{case})^2 th_{case} + \pi l_{tubes}\left((r_{net} + th_{case})^2 - r_{net}^2\right)\right) \tag{30}$$

$$m_{sys} = m_{Li} + m_{tubes} + m_{case} \tag{31}$$

As the pressure and volume of the tank are varied, the mass will also vary. The tank mass can be found from the tank volume, V_{tank},

$$r_{tank} = \left(\frac{3V_{tank}}{4\pi}\right)^{\frac{1}{3}} \tag{32}$$

Then, given the yield stress of the tank walls, σ_y, the thickness of the tank, and in turn the shell volume and tank mass for overwrap percentage Ov can be calculated, for P_{tank} and σ_y in MPa,

$$th_{tank} = \frac{r_{tank} P_{tank}}{2\sigma_y} \tag{33}$$

$$V_{shell} = \frac{4}{3}\pi\left((r_{tank} + th_{tank})^3 - (r_{tank})^3\right) \tag{34}$$

$$m_{tank} = (1 + Ov) V_{shell} \rho_{shell} \tag{35}$$

With these masses, a total system dry mass can be determined for a given lithium block mass and length, and a given tank volume and pressure.

$$m_{dry} = m_{base} + m_{sys} + m_{tank} \tag{36}$$

where m_{base} is the dry mass of the vehicle without the tank or lithium block assembly.

C. Optimization Results

Multiple simulations were performed in GFSSP for inputs into the MATLAB optimization system. An initial guess for the optimum case was a tank with initial conditions of 6000 psia, 300 K, and 0.465 m^3, and a lithium block mass of 40 kg. The initial optimization runs quickly shifted the guess for the initial tank pressure to 3000 psia, and with an assumed constant initial propellant mass, a new tank volume of 0.712 m^3. Optimizations were run for varying tank pressures, temperatures, and lithium masses assuming a constant total propellant load. The simulations would be cut off when either the remaining pressure was no longer sufficient to drive the 0.9 kg/s through the engine, or when the fluid in the tank reached saturation, as liquid nitrogen caused instabilities in the heat exchanger. This results in unused residual propellant. The results for these optimizations are provided in Appendix A, recorded in Tables 7, 8, and 9, and plotted in Figures 23 – 49, with the initial guess shown with the dotted line.

In addition, the GFSSP results tended to not reach the solidification point of the lithium block. While the latent heat would be a significant benefit to providing consistent performance, the relatively low solidification temperature of the lithium resulted in somewhat low performance during solidification, with fully liquid states providing higher performance. As such, it was not considered necessary to design to incorporate the phase change, instead relying on identifying the system optimum. The majority of the high performing configurations never reached solidification.

In particular, Figures 14 and 15, shown here, show the existence of an optimum hop distance for given tank conditions, with the 3000 psia and 300 K giving the greatest hop distance. However, since the initial optimizations were not based on any vehicle mass constraints, increasing the lithium mass simply increased hop distances, albeit with diminishing returns, as shown in Figure 16

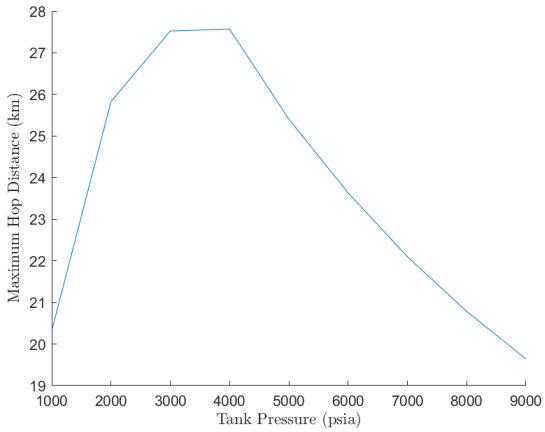

Fig. 14 Maximum Hop Distance with Variable Tank Pressure

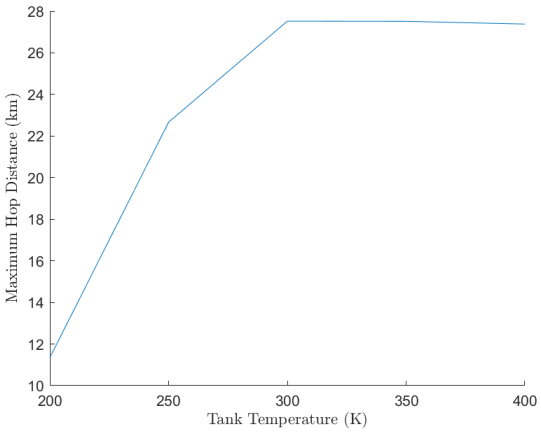

Fig. 15 Maximum Hop Distance with Variable Tank Temperature

To properly optimize the system, another constraint needed to be imposed. The total system mass, $m_{tank} + m_{sys}$, i.e., the vehicle dry mass, was fixed to the case for 3000 psia and 300 K. Then, by varying the lithium mass, a tank size could be determined to maintain the system mass. This way, an optimum could be found for the ideal nitrogen-to-lithium ratio for maximum hop distance. The same optimization was also run with a slightly lower dry mass, to verify if the optimum was indeed a ratio and not tied to the total dry mass. The results of these optimizations are also in Appendix A, in Tables 10 and 11, and Figures 50 – 67. As seen in Figures 17 and 18, such an optimum does exist; a nitrogen-to-lithium ratio of approximately 9.5. As such, a new system design point was chosen to maximize the hop distance, with the higher system mass, and characteristics and performance listed in Table 5.

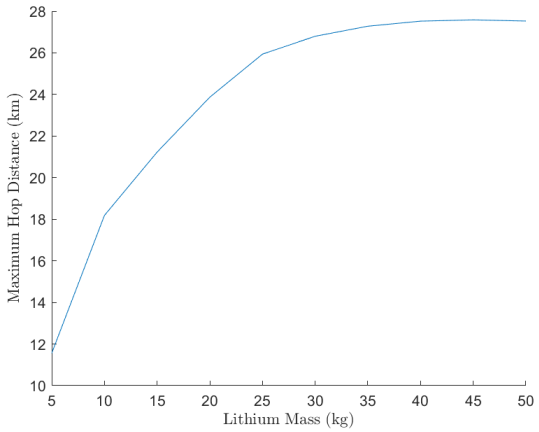

Fig. 16 Maximum Hop Distance with Variable Lithium Mass

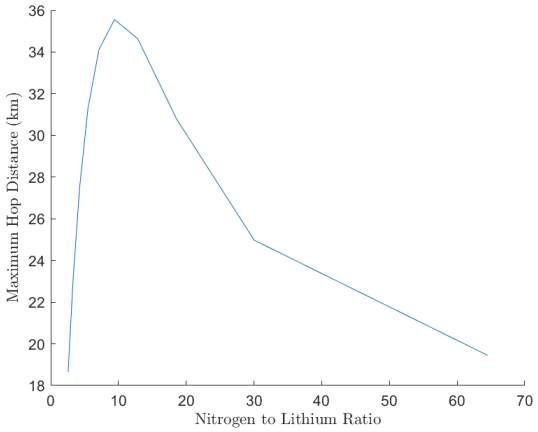

Fig. 17 Maximum Hop Distance with Variable Tank Pressure

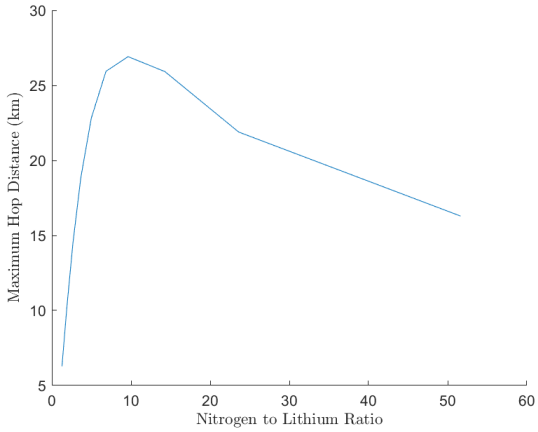

Fig. 18 Maximum Hop Distance with Variable Tank Temperature

Table 5 Optimum Configuration Parameters

Lithium Mass [kg]	Li Temperature [K]	Tank Pressure [psia]	Tank Temperature [K]	Tank Volume [m^3]
25	1473.15	3000	300	1.0753
Filled Propellant Mass [kg]	**Unused Propellant [kg]**	**Tank Mass [kg]**	**Lithium Assembly Mass [kg]**	**Hop Distance [km]**
235.26	28.02	59.42	38.64	39.52

V. Physical Design

This system has many physical design considerations as well. These include heat leaks through the system, insulation for the tank and heat exchanger, heat exchanger tank and piping materials, and the geometric layout of the heat exchanger.

A. Insulation Considerations

The parameters of this mission provide an interesting design challenge in terms of insulation. During operation of the heat exchanger, it is ideal to insulate the tank as much as possible. Meanwhile, it is required to cool the tank during

propellant collection, while also insulating and heating it during propellant storage. For most spaceflight missions, the vacuum of space only requires multi-layer insulation (MLI) to insulate the vehicle and this is also true during the flight to Triton. However, MLI can only insulate in a total vacuum. Even the extremely thin atmosphere of Triton is enough to spoil the performance of MLI. Consequently, the heat exchanger tank will be wrapped in MLI, then the entire casing assembly will be stored in a vacuum insulated chamber. Additionally, an analysis to calculate the heat loss of thermal block was conducted. The results are shown in Figure 19. Approximately 350W of thermal energy will leak from the system. Since each GPHS unit outputs 250W, this is equal to about one and a half units. For this reason, a total of four GPHS units are included in this design; two are dedicated to the thermal block, with the remaining two used for the Stirling engines.

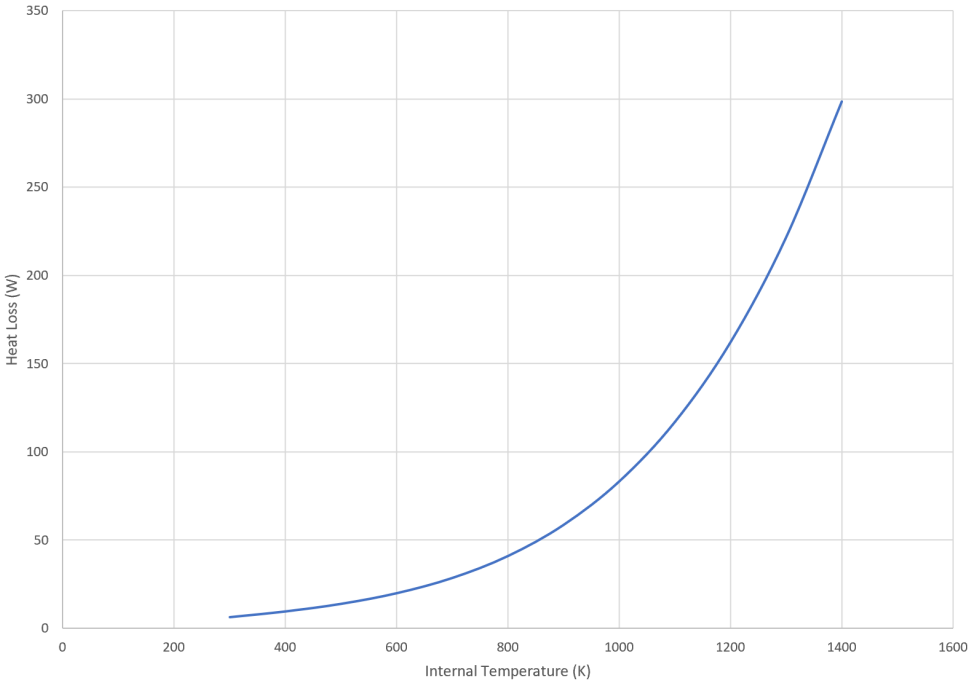

Fig. 19 Heat Exchanger Heat Loss to the Surroundings
90 Layers of MLI, 36 K Sink Temp

B. Heat Exchanger Piping Material

The Triton Hopper will contain a fairly unique form of energy storage — a mass of liquid lithium. This mass will be heated to temperatures as high as 1200 °C, at which point the cool nitrogen gas will flow through hundreds of small pipes surrounded by the lithium, heating the propellant. One of the concerns of this process is the material selection for the pipes themselves. The material must have a high melting point and good thermal conductivity to be able to achieve the best heat transfer results. Of course, the material must also be physically and chemically compatible with lithium as well. At these temperature ranges, these conditions limit the available materials.

One of the main limiting factors for the material selection is the maximum operating temperature of the material. Clearly, the melting point of the material must be considerably higher than the operating temperature of the system, 1200 °C. This parameter generally limits the selection of materials to refractory metals and their alloys, as well as stainless steel and superalloys. Another consideration is the thermal conductivity of the pipes, although, since the walls of the pipes will be thin, this parameter won't have a huge impact on the system. Nevertheless, the only refractory metals with a thermal conductivity above $100 \frac{\mathrm{W}}{\mathrm{m} \cdot \mathrm{K}}$ are Tungsten and Molybdenum. For comparison, the thermal conductivity of copper is $401 \frac{\mathrm{W}}{\mathrm{m} \cdot \mathrm{K}}$.

While this system is not technically a heat pipe system, many of the design considerations are the same. Several studies have been done for heat pipes operating in this temperature range with lithium as the working fluid. A compatibility study at Wright AF Aeronautical Laboratory tested lithium heat pipes with several superalloys, such as

Stainless Steel 304L and 310S, Hastalloy X and B, and Haynes 183. All these alloys were found to be incompatible with lithium. Additionally, these alloys also have melting temperature ranges with minimum values within only a few hundred degrees of our operating temperature[4].

According to Advanced Cooling Technologies (ACT), refractory metals have much better mechanical properties at high temperatures[5]. Further research indicates that there is a preferred alloy for lithium heat pipes — Titanium Zirconium Molybdenum (TZM). This material has a high melting point, 2500 – 3600 °C, a high thermal conductivity for high-temperature materials, $110 \frac{W}{m \cdot K}$ at 1000 °C, and has a high strength. TZM is mostly comprised of molybdenum, but performs better than molybdenum itself. This is due to the fact that, at high temperatures, TZM forms carbides which prevents re-crystallization in the material, resulting in better mechanical properties. It is also the mostly widely used molybdenum alloy. ACT constructed a test stand for a TZM heat pipe operating in a vacuum environment, seen in Figure 20.

Another study from Los Alamos National Lab tested several materials for use in a heat pipe system for a space reactor core[6]. The study examined several materials, including TZM. TZM was found to be a high performing material, especially considering the high creep strength, potentially allowing weight saving opportunities. TZM tubing is also arc cast and widely available. In a NASA study for heat pipe cooling of scramjet engines, a TZM and Li system was implemented[7]. Generally, in a lithium heat pipe system, TZM is one of the most common materials.

Fig. 20 TZM-Li Heat Pipe

C. Heat Exchanger Geometry Layout

The interior geometry of the heat exchanger is another important design point. Heat must be able to transfer as symmetrically as possible throughout the lithium mass to enable the maximum possible efficiency. For this to happen, the heat transfer pipes themselves must be placed in a strategic fashion, with the goal being that each pipe receives the same amount of heat. Of course, the pipes must fit within the lithium mass itself, while at the same time avoiding 'crowding' of the pipes. With that in mind, a geometry consisting of sets of concentric rings was designed, shown in Figure 21. The inner ring consists of 36 pipes, with each outer ring consisting of 6 additional elements. The center of the block contains a rectangular slot. This is where the 4 GPHS units will reside. Containing them within the lithium block itself allows for direct heat transfer to the block to occur, providing a quicker heating time.

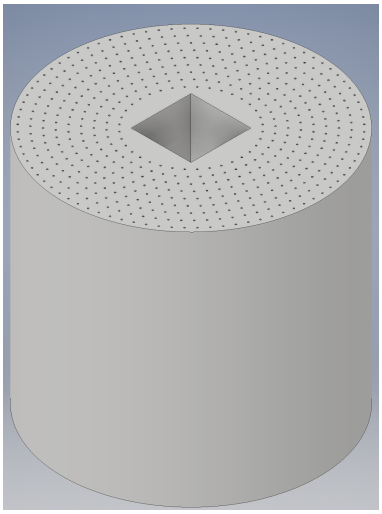

Fig. 21 Autodesk Inventor Model of the Heat Exchanger

VI. Conclusion

Analysis of a Radioisotope Heat Exchanger Rocket not only determined that such a vehicle is possible, it has shown that the vehicle can operate efficiently and allow for a depth of exploration that no other vehicle has achieved on the surface of another celestial body. The addition of a radioisotope heat source combined with a lithium thermal mass has drastically improved the capabilities of the vehicle over the previous design, as seen in Table 6[8]. The vehicle can not only hop longer distances, it can do so in a shorter amount of time with improved engine efficiency. In fact, for a two year mission, this vehicle can hop from the south pole of Triton to the equator, plus an additional 300 km. The vehicle will explore over one hundred different sites in one mission in a relatively short span of time, ultimately saving time and money. While this research has primarily focused on Triton as the exploratory body, the mission concept can be applied to any planet or moon with an atmosphere or surface that can be used as fuel. Future research of this concept should consist of beginning laboratory experimentation of the heat exchanger. A test stand should be created with a scale model of the heat exchanger and rocket, verifying the data gathered from the GFSSP, MATLAB, and ANSYS simulations.

Table 6 Phase I vs Phase II Design

Mission Parameters	Phase I: Cold Gas Rockets	Phase II: Pu^{238} rocket	Improvement
Science	29 kg, 30 sites	43 kg, 120 sites	1.5X mass, 4X sites
Hop Length	5 km	20 km	4X
Hop Frequency	Every 24 Days	Every 6 Days	4X
Total Distance (2 years)	150 km	2400 km	16X
Dry Mass	360 kg	470 kg	Increase of 110 kg
Usable N2 Hop Propellant	100 kg	137 kg	1.4X
Comm Frequency	Flyby Every 24 Days	Flyby Every 3 Days	8X
Comm Distance	210,0000 km	241 km	1000X

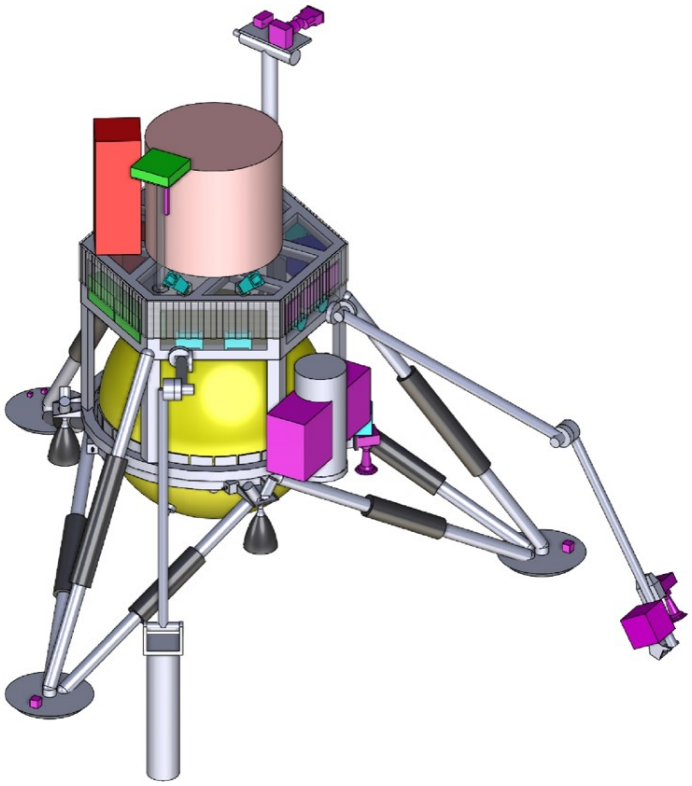

Fig. 22 CAD Model of Triton Hopper

Appendix

A. Raw Data

Table 7 Performance with varying initial tank pressure

Tank Pressure [psia]	Tank Mass [kg]	Lithium Assembly Mass [kg]	Tank Residuals [kg]	Hop Distance [km]	Average I_{sp} [s]
1000	40.38	54.90	46.66	24.53	153.18
2000	41.34	54.90	29.71	29.11	149.77
3000	43.17	54.90	23.96	30.30	148.21
4000	45.64	54.90	22.55	30.17	147.44
5000	48.56	54.90	27.35	28.32	147.77
6000	51.78	54.90	31.31	26.74	148.03
7000	55.16	54.90	34.81	25.33	148.28
8000	58.67	54.90	37.86	24.09	148.51
9000	62.24	54.90	40.57	22.98	148.71

Table 8 Performance with varying initial tank temperature

Tank Temperature [K]	Tank Mass [kg]	Lithium Assembly Mass [kg]	Tank Residuals [kg]	Hop Distance [km]	Average I_{sp} [s]
200	24.80	54.90	76.70	15.53	150.74
250	34.27	54.90	37.74	26.45	147.81
300	43.17	54.90	23.96	30.30	148.21
350	51.51	54.90	23.79	30.23	150.40
400	59.47	54.90	23.85	30.05	152.41

Table 9 Performance with varying Lithium Masses

Lithium mass [kg]	Tank Mass [kg]	Lithium Assembly Mass [kg]	Tank Residuals [kg]	Hop Distance [km]	Average I_{sp} [s]
5	43.17	16.62	18.36	12.52	85.08
10	43.17	22.20	18.15	19.66	107.80
15	43.17	27.72	20.16	23.12	119.65
20	43.17	33.19	20.51	26.01	128.66
25	43.17	38.64	21.61	28.37	136.77
30	43.17	44.08	22.61	29.40	141.64
35	43.17	49.49	23.38	30.00	145.33
40	43.17	54.90	23.96	30.30	148.21
45	43.17	60.39	24.46	30.40	150.52
50	43.17	65.68	24.85	30.35	152.41

Table 10 Performance with varying Nitrogen to Lithium Ratio

N_2 to Li Ratio	Tank Mass [kg]	Lithium Assembly Mass [kg]	Tank Residuals [kg]	Hop Distance [km]	Average I_{sp} [s]
2.56	32.38	65.68	19.18	20.21	156.76
3.32	37.77	60.29	21.75	25.37	152.87
4.27	43.17	54.90	23.96	30.30	148.21
5.49	48.57	49.49	25.72	34.62	142.55
7.13	53.99	44.08	26.95	37.85	135.64
9.41	59.42	38.64	28.02	39.52	127.45
12.84	64.87	33.19	28.52	38.49	116.49
18.57	70.35	27.72	31.75	34.55	103.90
30.03	75.86	22.20	34.57	28.24	88.76
64.49	81.44	16.62	37.27	22.14	74.56

Table 11 Performance with varying Nitrogen to Lithium Ratio — Lower System Mass

N_2 to Li Ratio	Tank Mass [kg]	Lithium Assembly Mass [kg]	Tank Residuals [kg]	Hop Distance [km]	Average I_{sp} [s]
1.28	16.13	65.68	9.86	6.57	163.63
1.89	21.52	60.29	12.94	10.82	160.29
2.66	26.92	54.90	15.77	15.62	156.23
3.66	32.32	49.49	18.26	20.40	151.20
4.98	37.74	44.08	20.27	24.86	144.86
6.84	43.17	38.64	21.61	28.37	136.77
9.62	48.62	33.19	22.52	29.49	125.18
14.28	54.09	27.72	23.48	28.45	111.95
23.60	59.61	22.20	26.60	24.27	95.95
51.62	65.19	16.62	29.27	18.21	77.53

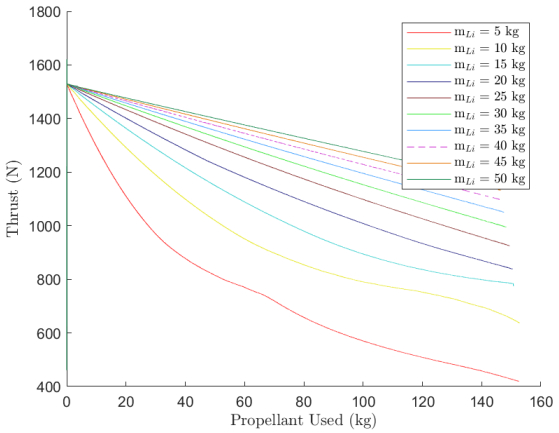

Fig. 23 Thrust with Variable Lithium Mass

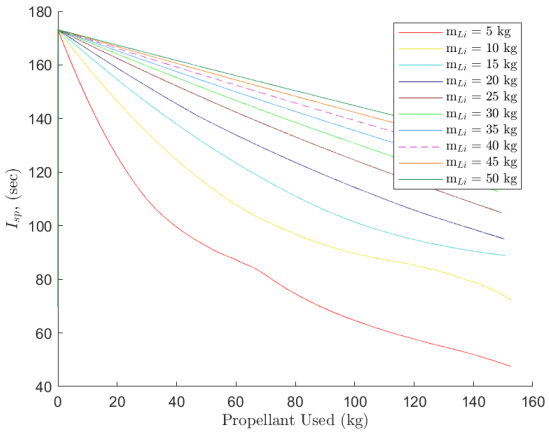

Fig. 24 I_{sp} with Variable Lithium Mass

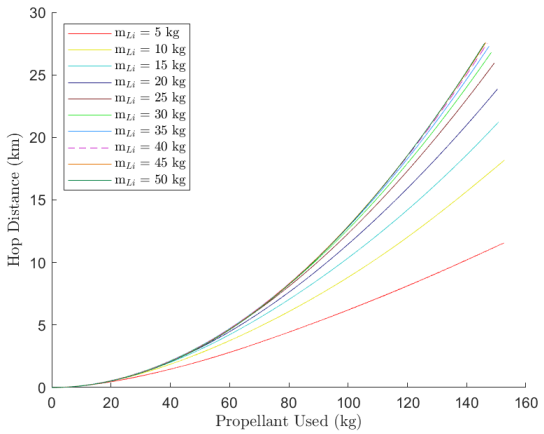

Fig. 25 Hop Distance Over Propellant Used with Variable Lithium Mass

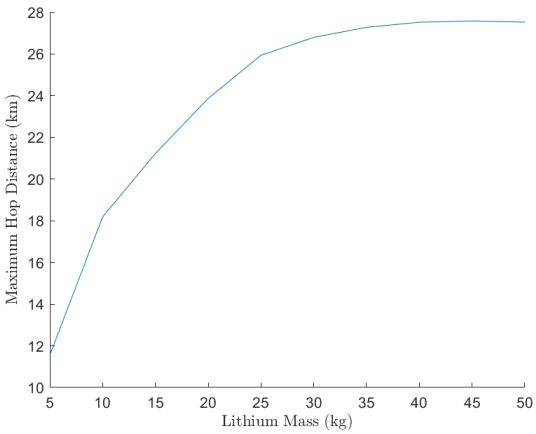

Fig. 26 Maximum Hop Distance with Variable Lithium Mass

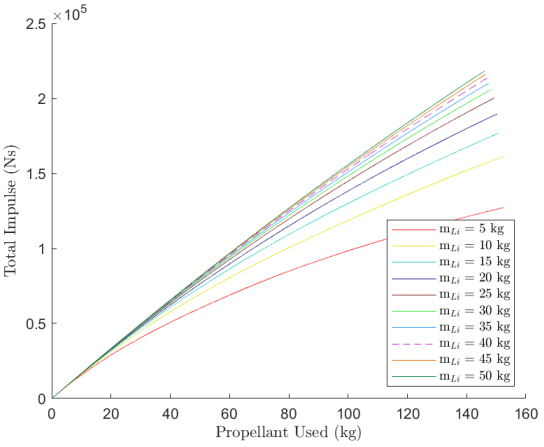

Fig. 27 Total Impulse with Variable Lithium Mass

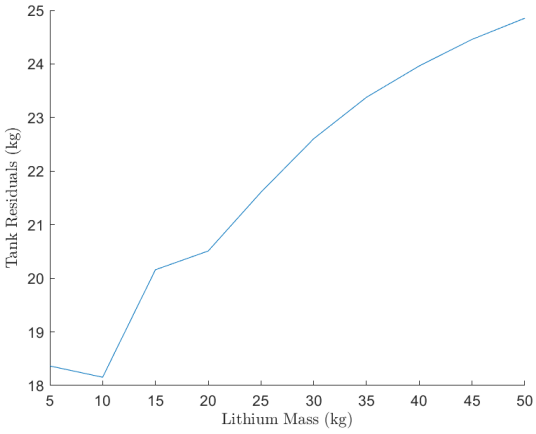

Fig. 28 Tank Residuals with Variable Lithium Mass

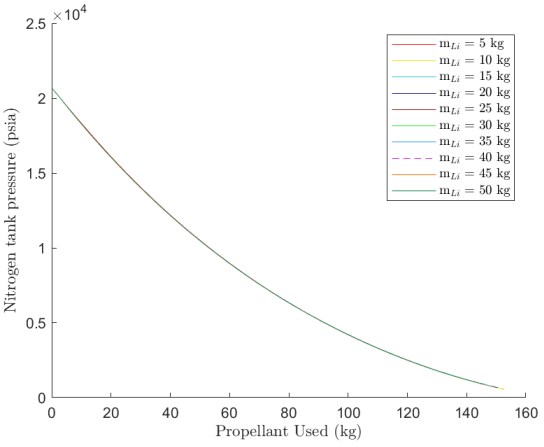

Fig. 29 Tank Pressure with Variable Lithium Mass

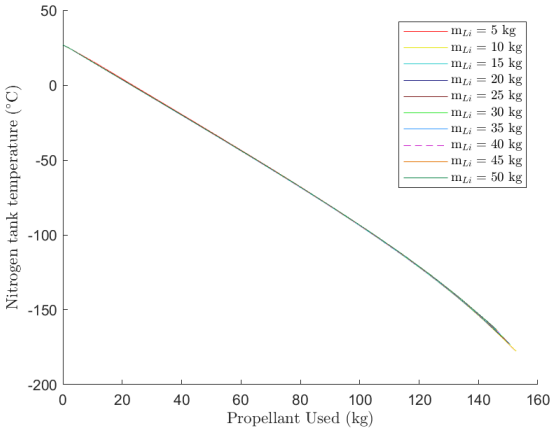

Fig. 30 Tank Temperature with Variable Lithium Mass

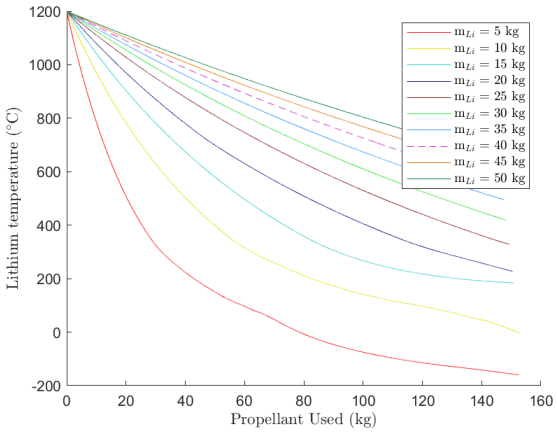

Fig. 31 Average Solid Temperature with Variable Lithium Mass

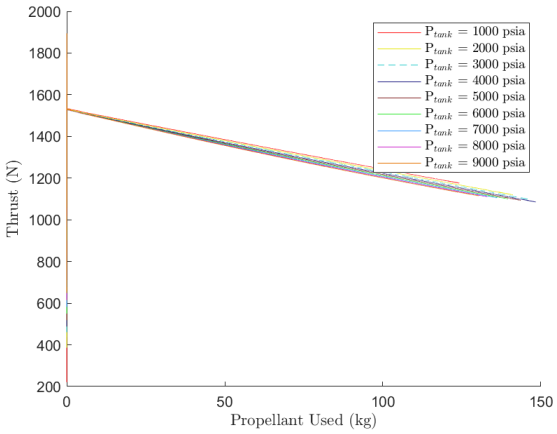

Fig. 32 Thrust with Variable Tank Pressure

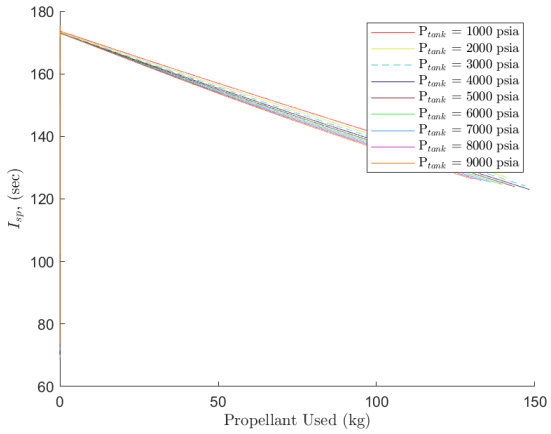

Fig. 33 I_{sp} with Variable Tank Pressure

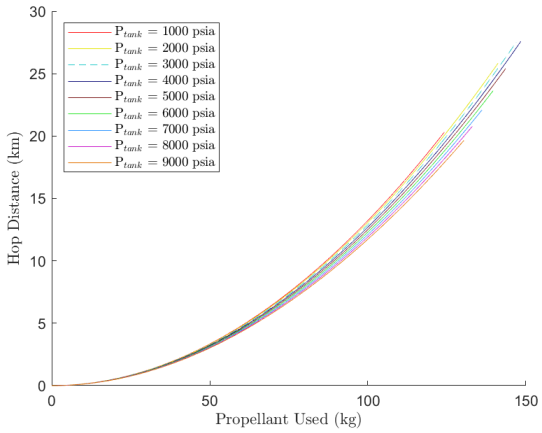

Fig. 34 Hop Distance Over Propellant Used with Variable Tank Pressure

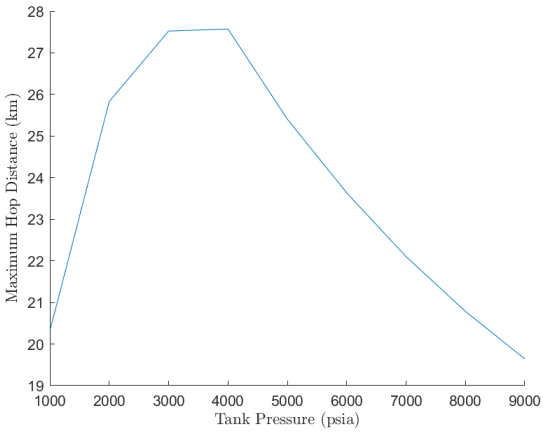

Fig. 35 Maximum Hop Distance with Variable Tank Pressure

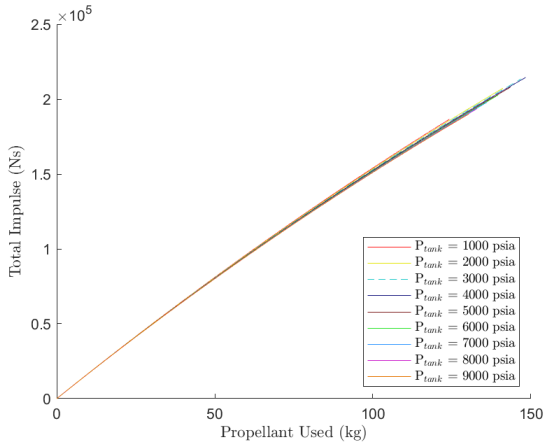

Fig. 36 Total Impulse with Variable Tank Pressure

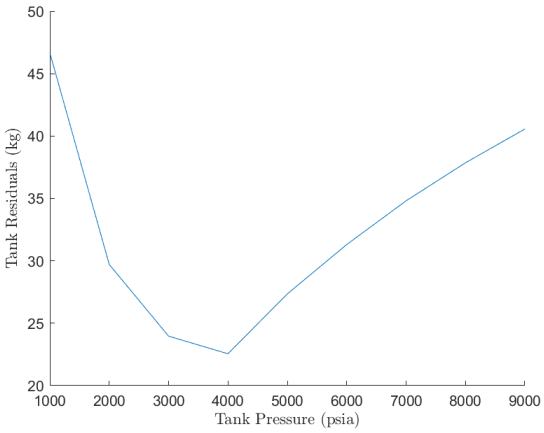

Fig. 37 Tank Residuals with Variable Tank Pressure

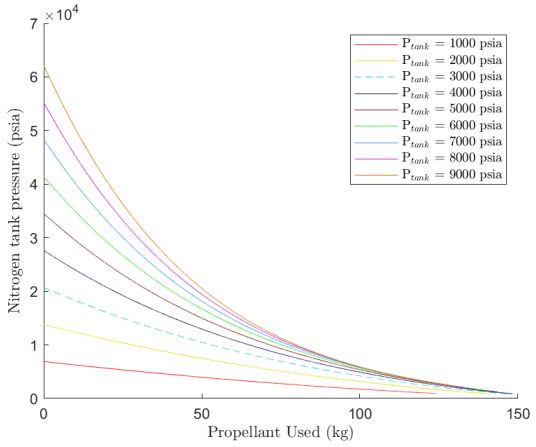

Fig. 38 Tank Pressure with Variable Tank Pressure

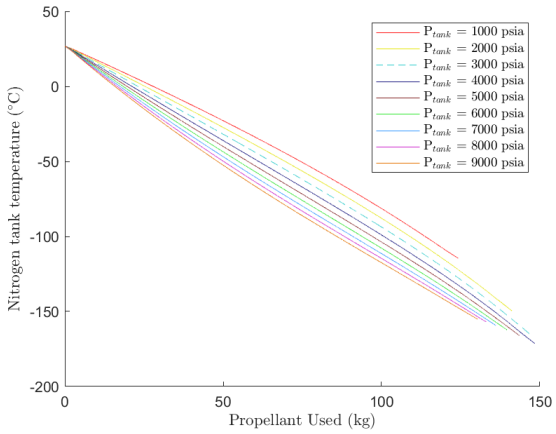

Fig. 39 Tank Temperature with Variable Tank Pressure

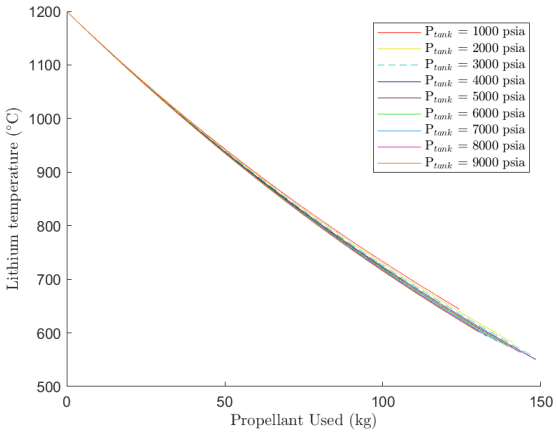

Fig. 40 Average Solid Temperature with Variable Tank Pressure

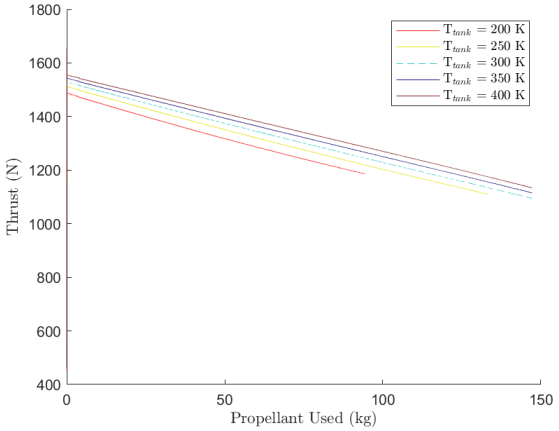

Fig. 41 Thrust with Variable Tank Temperature

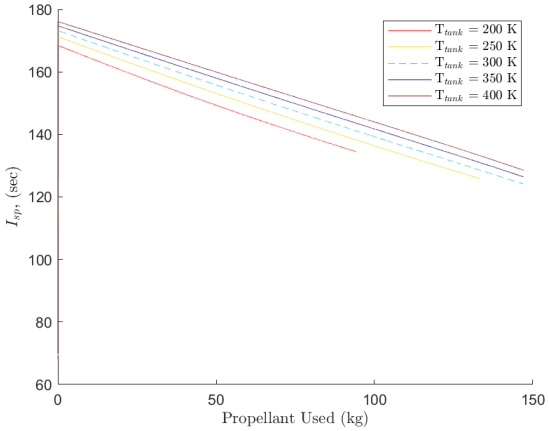

Fig. 42 I_{sp} with Variable Tank Temperature

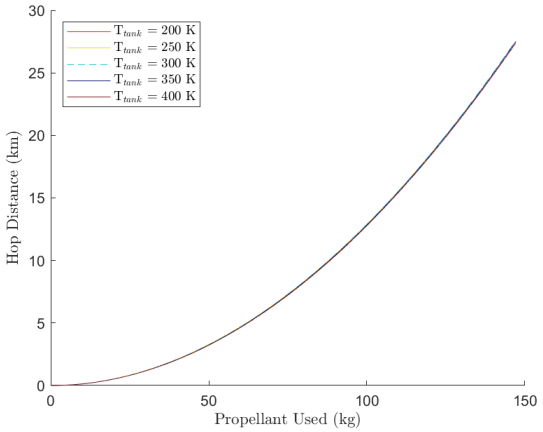

Fig. 43 Hop Distance Over Propellant Used with Variable Tank Temperature

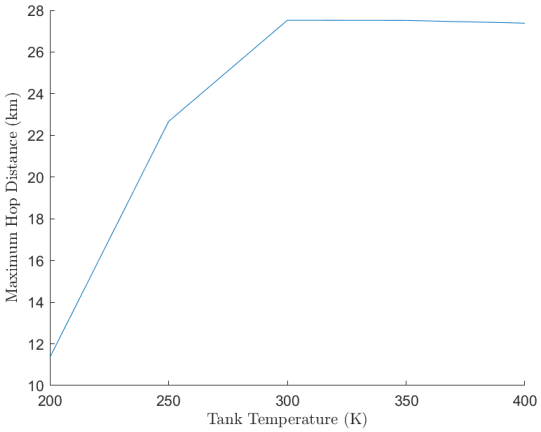

Fig. 44 Maximum Hop Distance with Variable Tank Temperature

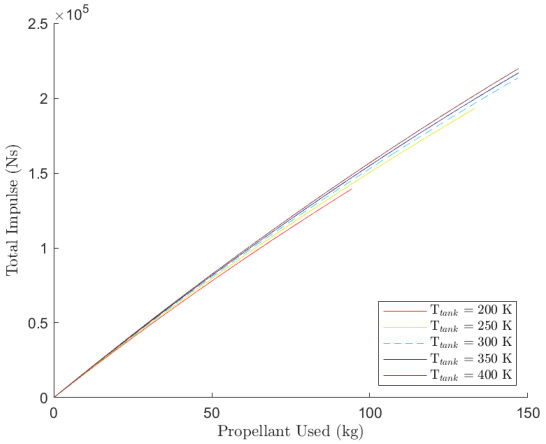

Fig. 45 Total Impulse with Variable Tank Temperature

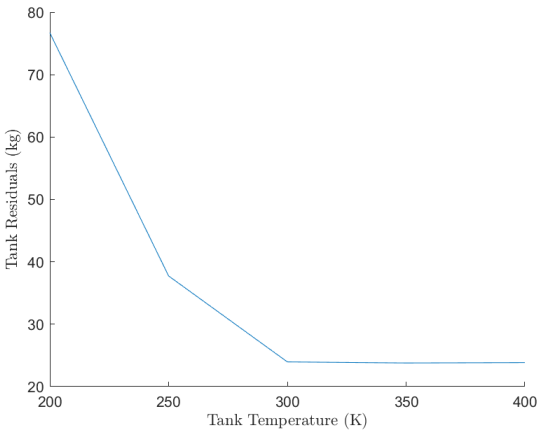

Fig. 46 Tank Residuals with Variable Tank Temperature

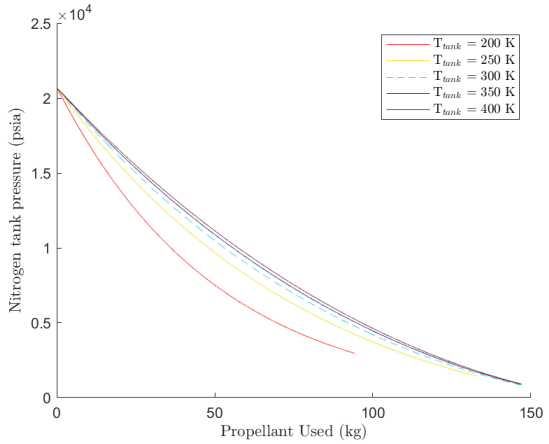

Fig. 47 Tank Temperature with Variable Tank Temperature

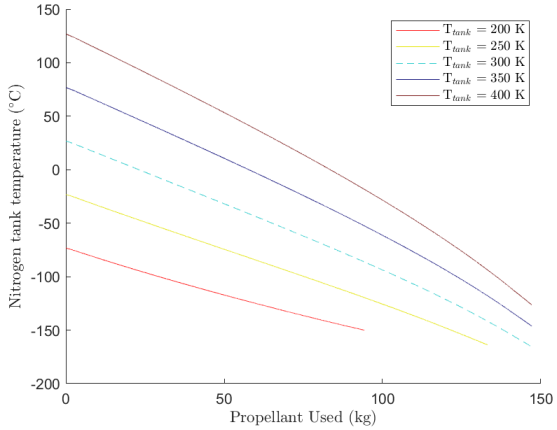

Fig. 48 Tank Temperature with Variable Tank Temperature

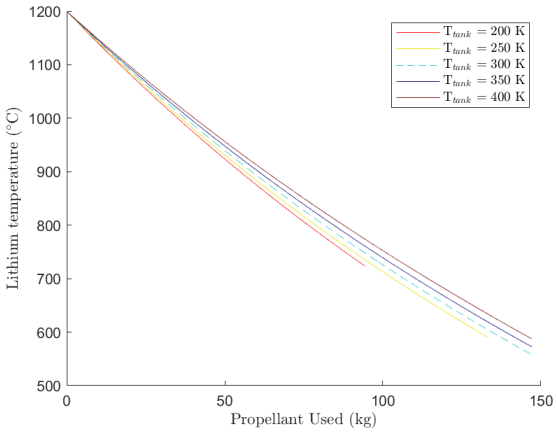

Fig. 49 Average Solid Temperature with Variable Tank Temperature

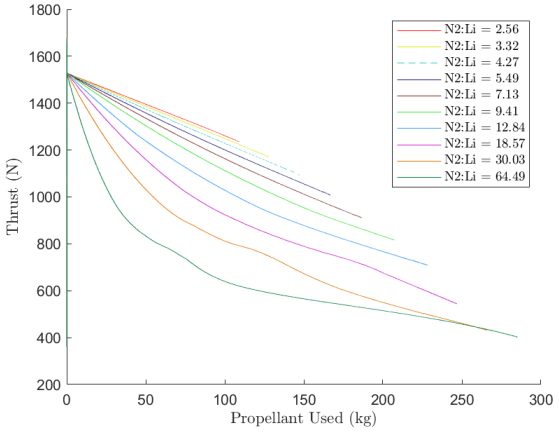

Fig. 50 Thrust with Variable N_2:Li Ratio

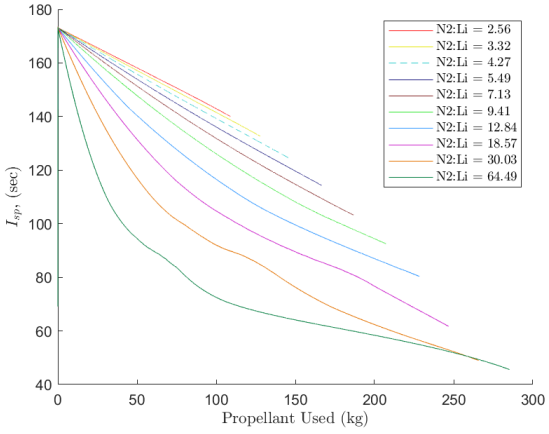

Fig. 51 I_{sp} with Variable N_2:Li Ratio

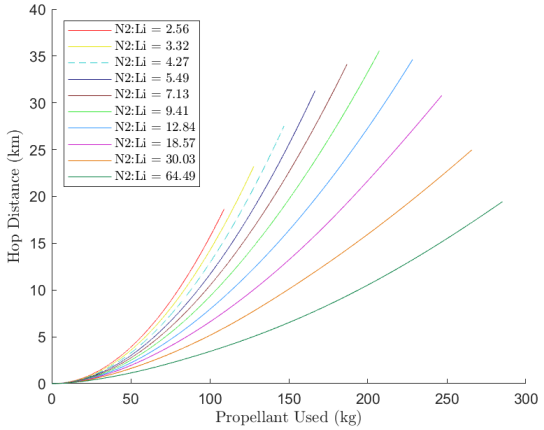

Fig. 52 Hop Distance Over Propellant Used with Variable N_2:Li Ratio

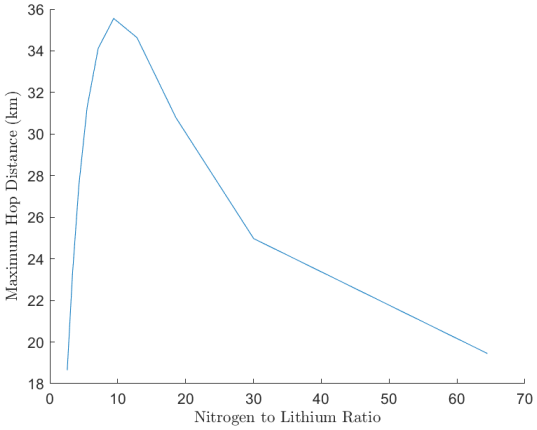

Fig. 53 Maximum Hop Distance with Variable N_2:Li Ratio

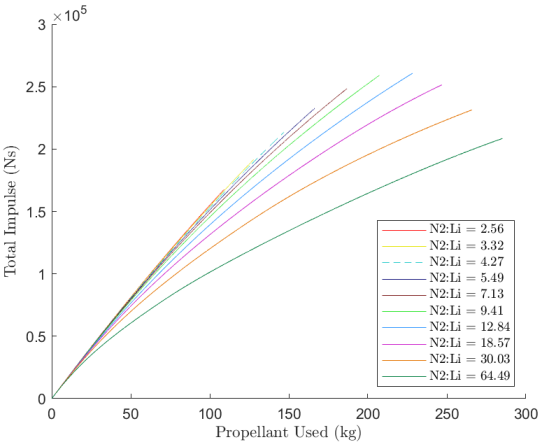

Fig. 54 Total Impulse with Variable N_2:Li Ratio

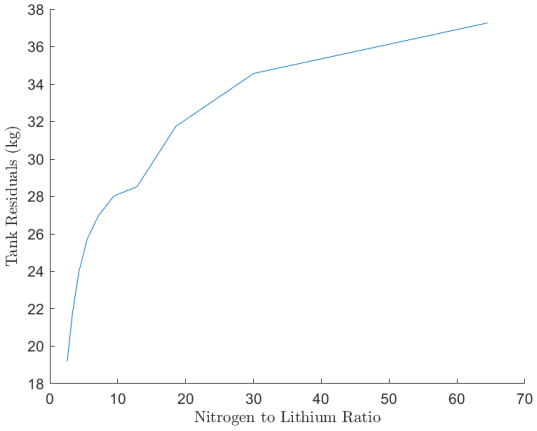

Fig. 55 Tank Residuals with Variable N_2:Li Ratio

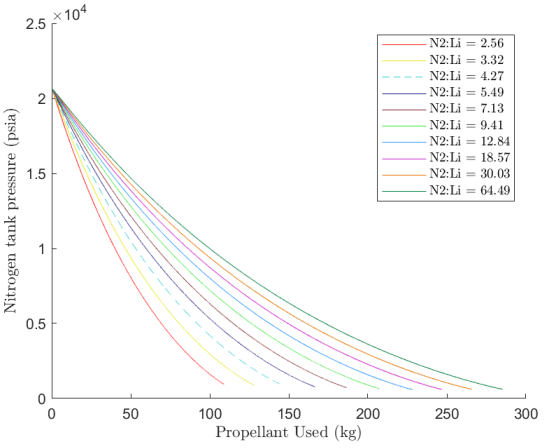

Fig. 56 N_2:Li Ratio with Variable N_2:Li Ratio

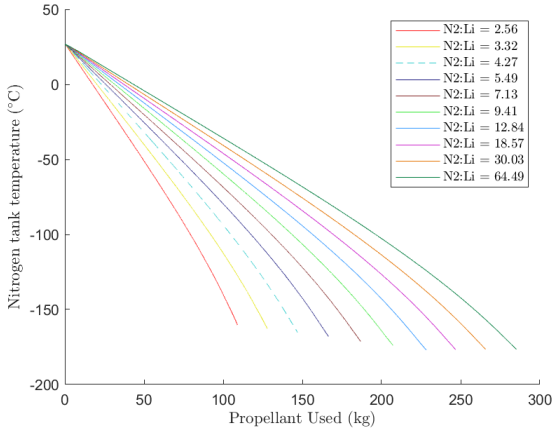

Fig. 57 N_2:Li Ratio with Variable N_2:Li Ratio

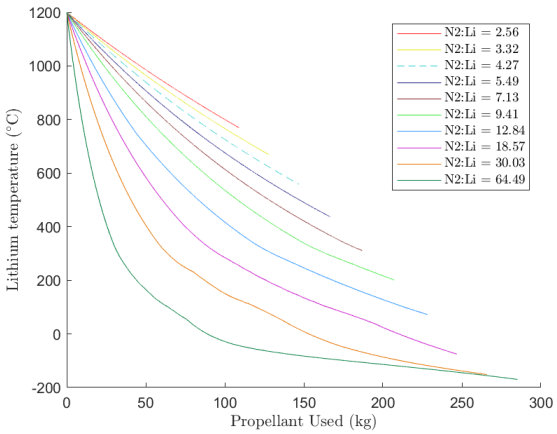

Fig. 58 Average Solid Temperature with Variable N_2:Li Ratio

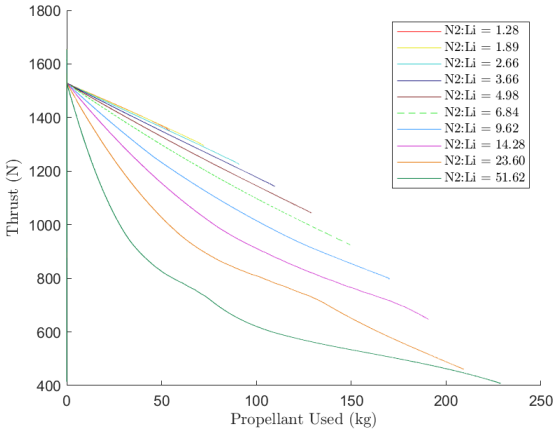

Fig. 59 Thrust with Variable N_2:Li Ratio — Lower System Mass

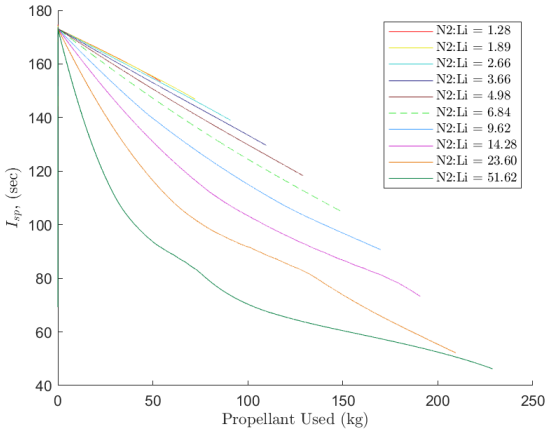

Fig. 60 I_{sp} with Variable N_2:Li Ratio — Lower System Mass

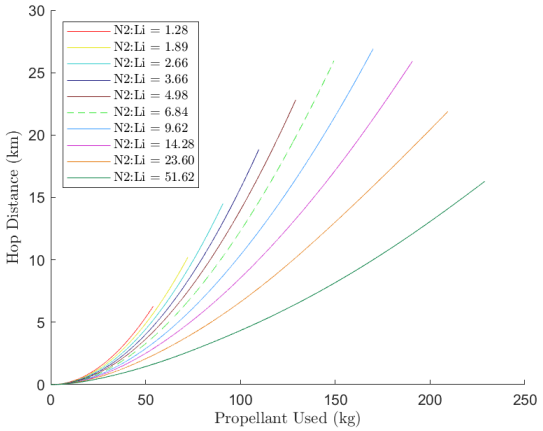

Fig. 61 Hop Distance Over Propellant Used with Variable N_2:Li Ratio — Lower System Mass

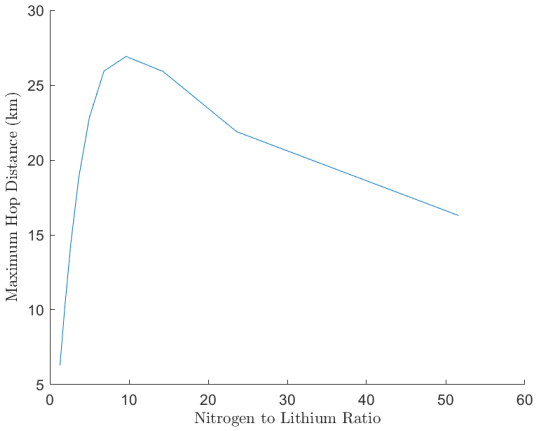

Fig. 62 Maximum Hop Distance with Variable N_2:Li Ratio — Lower System Mass

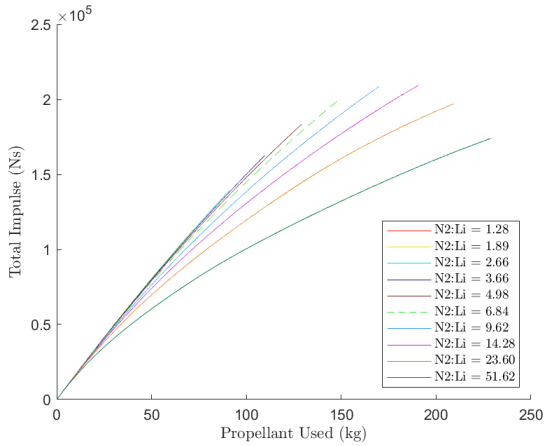

Fig. 63 Total Impulse with Variable N_2:Li Ratio — Lower System Mass

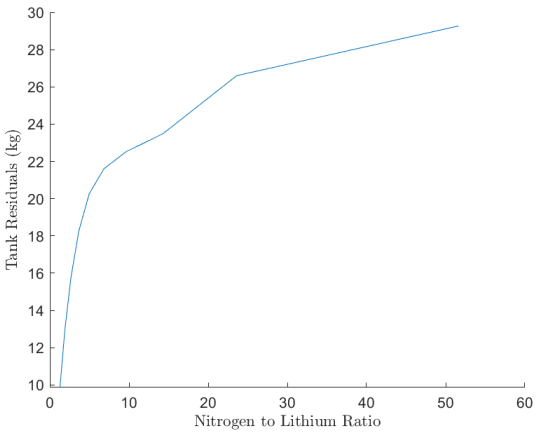

Fig. 64 Tank Residuals with Variable N_2:Li Ratio — Lower System Mass

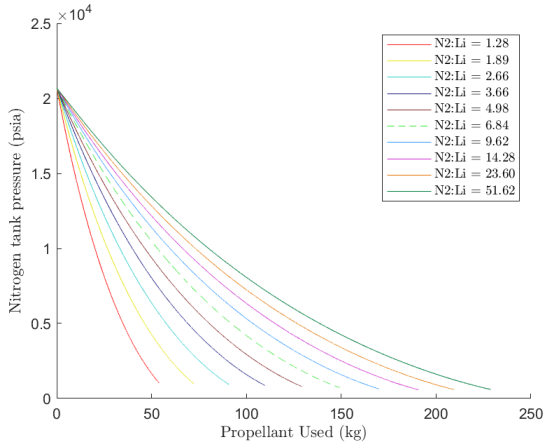

Fig. 65 N_2:Li Ratio — Lower System Mass with Variable N_2:Li Ratio — Lower System Mass

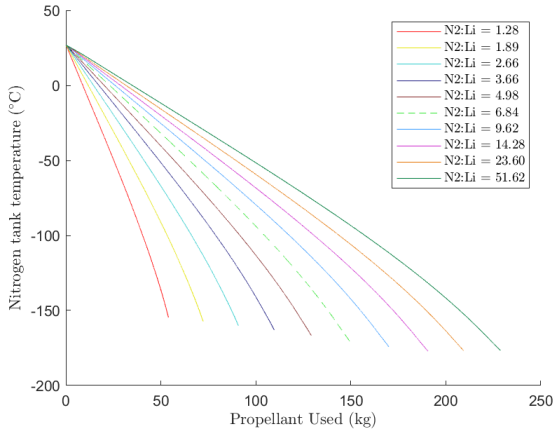

Fig. 66 N_2:Li Ratio — Lower System Mass with Variable N_2:Li Ratio — Lower System Mass

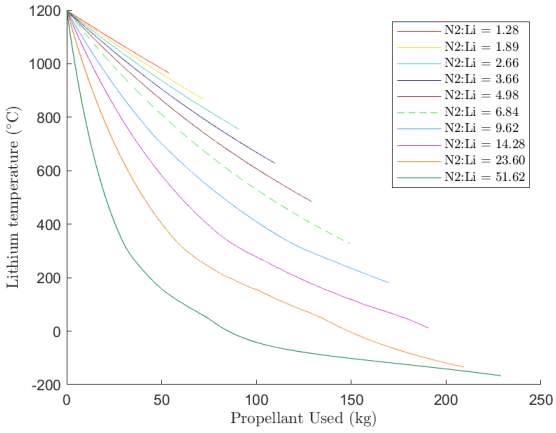

Fig. 67 Average Solid Temperature with Variable N_2:Li Ratio — Lower System Mass

B. Code

Listing 1 Code for determining hop distance from GFSSP outputs

```
clc; close all; clear all;

num = 9;    %Number of data sets
mLiList = [40, 40, 40, 40, 40, 40, 40, 40, 40]; %List of lithium block masses, [kg]
PressList = [3000, 1000, 2000, 4000, 5000, 6000, 7000, 8000, 9000]; %List of initial tank pressures, [psia]
TList = [300, 300, 300, 300, 300, 300, 300, 300, 300];  %List of initial tank temperatures, [K]
VList = [0.7812, 2.203, 1.125, 0.6179, 0.5247, 0.465, 0.4236, 0.3932, 0.3699];  %List of tank volumes, [m^3]
rhoList = zeros(1,numel(PressList));    %Initialize array
for i = 1:numel(PressList)
    rhoList(i) = refpropm('D','T',TList(i),'P',PressList(i)*6.89476,'nitrogen');    %Calculate initial densities from REFPROP, [kg/m^3]
end
mN2List = VList.*rhoList;   %Create list of initial nitrogen mass in tanks, [kg]

ColorList = [255,26,26; 229,230,12; 41,204,204; 26,25,128; 127,32,32; 46,230,46; 51,153,255; 204,31,204; 229,115,0; 6,128,67; 13,13,255; 255,0,128]/255; %List of colors for plotting

g = 9.80665;    %Gravitational acceleration on Earth, [m/s^2]
gt = 0.779; %Gravitational acceleration on Triton, [m/s^2]
dt = 0.01;      %Time step, seconds
R = 296.8;      %Nitrogen Gas Constant, [J/kg-K]
lTube = .35;    %Tube Length, [m]
diTube = .0015; %Tube Inner Diameter, [m]
doTube = .003;  %Tube Outer Diameter, [m]
rhoTube = 10200;        %Density of Tubes, [kg/m^3]
nTube = 540;    %Number of tubes
mBlock = mLiList;       %Mass of Thermal Block, [kg]
rhoBlock = 534; %Density of Thermal Block, [kg]
rhoCase = 4506; %Density of Casing, [kg/m^3]
tCase = .001;   %Thickness of Casing, [m]
nGPHS = 4;      %Number of GPHS blocks

mGPHS = 1.5;    %Mass of GPHS block, [kg]
VGPHS = .1*.1*.05;      %Volume of GPHS block, [m^3]

mBase = 315;    %Dry mass of vehicle without tank or lithium block assembly

yTank = 1378.952;   %Yield strength of tank wall, [MPa]
rhoShell = 2216;    %Density of tank wall, [kg/m^3]
Overwrap = .1;  %Overwrap offset

FN = cell(num,1);   %Initialize cell arrays for iterations
Br = cell(num,1);
SN = cell(num,1);

Time = cell(num,1);
Pc = cell(num,1);
Tc = cell(num,1);
Vc = cell(num,1);
mdotc = cell(num,1);
TS = cell(num,1);
Tt = cell(num,1);
Pt = cell(num,1);
Gamc = cell(num,1);
```

```
ac = cell(num,1);
Mc = cell(num,1);
T0c = cell(num,1);
ue = cell(num,1);
F = cell(num,1);
Isp = cell(num,1);
I = cell(num,1);
mProp = cell(num,1);
Tavg = cell(num,1);
HopDist = cell(num,1);
avgIsp = zeros(num,1);

mTube = (nTube*lTube*pi/4*(doTube^2-diTube^2))*rhoTube; %Mass of heat exchanger tubes [kg]
VBlock = mBlock/rhoBlock;   %Volume of lithium block, [m^3]
VNet = VBlock+nGPHS*VGPHS+nTube*lTube*pi/4*doTube^2;    %Total volume of lithium, tubes, and GPHS
    blocks, [m^3]
rNet = sqrt(VNet/(lTube*pi));   %Radius of lithium block, [m]
mCase = rhoCase*(2*pi*(rNet+tCase).^2*tCase+lTube*pi*((rNet+tCase).^2-rNet.^2));    %Mass of thermal
    block casing, [kg]]
mSys = mTube+mBlock+mCase;  %Thermal block assembly mass, [kg]

rTank = (VList/pi/4*3).^(1/3);  %Radius of tank, [m]
tTank = rTank.*PressList*6.89476/1000/yTank/2;  %Thickness of tank, [m]
vShell = 4/3*pi*((rTank+tTank).^3-(rTank).^3);  %Volume of tank shell, [m^3]
mTank = (1+Overwrap)*vShell*rhoShell;   %Mass of tank, [kg]

mDry = mBase+1*mTank+mSys;  %Total system dry mass, [kg]

for j = 1:num
    FNFileName = sprintf('exhaustFN%d.CSV',j);  %Initialize file names
    BrFileName = sprintf('exhaustB%d.CSV',j);
    SNFileName = sprintf('exhaustSN%d.CSV',j);

    FN{j} = readmatrix(FNFileName); %Read GFSSP outputs
    Br{j} = readmatrix(BrFileName);
    SN{j} = readmatrix(SNFileName);

    Time{j} = FN{j}(:,1);   %Pull required data into smaller arrays
    Pc{j} = FN{j}(:,14);
    Tc{j} = FN{j}(:,28)+273.15;
    Tt{j} = FN{j}(:,16);
    Pt{j} = FN{j}(:,2);
    Vc{j} = Br{j}(:,26);
    mdotc{j} = Br{j}(:,14);
    TS{j} = SN{j}(:,13:23);

    Gamc{j} = zeros(numel(Pc{j}),1);    %Initialize specific heat ratio array
    for i=1:numel(Pc{j})
        Gamc{j}(i) = refpropm('K','T',Tc{j}(i),'P',Pc{j}(i),'nitrogen');    %Pull specific heats from
            REFPROP
        %Gamc{j}(i) = 1.4;
    end

    ac{j} = sqrt(Gamc{j}.*R.*Tc{j});    %Calculate chamber inlet speed of sound at each time step, [m/
        s]
    Mc{j} = Vc{j}./ac{j};   %Calculate chamber inlet Mach number at each time step
    T0c{j} = Tc{j}.*(1+(Gamc{j}-1)./2.*Mc{j}.^2);   %Calculate total chamber temperature at each time
        step, [K]
```

```
    ue{j} = sqrt((2*Gamc{j}.*R.*T0c{j})./(Gamc{j}-1));  %Calculate nozzle exit velocity at each time step, [m/s]

    F{j} = mdotc{j}.*ue{j}*.94; %Calculate thrust at each time step, [N]
    Isp{j} = ue{j}/g*.94;   %Calculate specific impulse at each time step,[s]

    I{j} = zeros(numel(Pc{j}),1);   %Initialize additional arrays
    mProp{j} = zeros(numel(Pc{j}),1);
    Tavg{j} = zeros(numel(Pc{j}),1);
    I{j}(1) = dt/2*F{j}(1);
    mProp{j}(1) = dt/2*mdotc{j}(1);
    Tavg{j}(1) = mean(TS{j}(1,:));
    for i = 2:numel(Pc{j})
        I{j}(i) = I{j}(i-1) + dt/2*(F{j}(i)+F{j}(i-1)); %Integrate total impulse by trapezoid method
        mProp{j}(i) = mProp{j}(i-1) + dt/2*(mdotc{j}(i)+mdotc{j}(i-1)); %Integrate propellant used by trapezoid method
        Tavg{j}(i) = mean(TS{j}(i,:));  %Store average lithium temperatures
    end
    HopDist{j} = (I{j}./(mDry(j)+max(mProp{j})-mProp{j}/2)*0.7).^2/(4*gt)/1000; %Approximate hop distance based on delta-V
    avgIsp(j) = mean(Isp{j});   %Save average Isp
end
[~,ind] = sort(PressList);  %Sort by increasing pressures, save a list of indices for later use

leg = cell(num,1);

ax1 = figure(1);
hold on
for k = 1:num   %Plot in increasing order of pressure
    j = ind(k);
    if j == 1
        plot(mProp{j},F{j},'--','Color',ColorList(k,:))
    else
        plot(mProp{j},F{j},'Color',ColorList(k,:))
    end
    leg{k} = sprintf('P$_{tank}$ = %d psia',PressList(j));
end
legend(leg,'Interpreter','latex')
xlabel('Propellant Used (kg)','Interpreter','latex')
ylabel('Thrust (N)','Interpreter','latex')
title('Hopper Thrust over Propellant Used','Interpreter','latex')
hold off

ax2 = figure(2);
hold on
for k = 1:num   %Plot in increasing order of pressure
    j = ind(k);
    if j == 1
        plot(mProp{j},Isp{j},'--','Color',ColorList(k,:))
    else
        plot(mProp{j},Isp{j},'Color',ColorList(k,:))
    end
end
legend(leg,'Interpreter','latex')
xlabel('Propellant Used (kg)','Interpreter','latex')
ylabel('$I_{sp}$, (sec)','Interpreter','latex')
title('Hopper Specific Impulse over Propellant Used','Interpreter','latex')
hold off

```

```
ax3 = figure(3);
hold on
for k = 1:num   %Plot in increasing order of pressure
    j = ind(k);
    if j == 1
        plot(mProp{j},I{j},'--','Color',ColorList(k,:))
    else
        plot(mProp{j},I{j},'Color',ColorList(k,:))
    end
end
legend(leg,'Location','southeast','Interpreter','latex')
xlabel('Propellant Used (kg)','Interpreter','latex')
ylabel('Total Impulse (Ns)','Interpreter','latex')
title('Hopper Total Impulse over Propellant Used','Interpreter','latex')
hold off

ax4 = figure(4);
hold on
for k = 1:num   %Plot in increasing order of pressure
    j = ind(k);
    if j == 1
        plot(mProp{j},Tavg{j},'--','Color',ColorList(k,:))
    else
        plot(mProp{j},Tavg{j},'Color',ColorList(k,:))
    end
end
legend(leg,'Interpreter','latex')
xlabel('Propellant Used (kg)','Interpreter','latex')
ylabel('Lithium temperature ($^{\circ}$C)','Interpreter','latex')
title('Lithium Average Temperature over Propellant Used','Interpreter','latex')
hold off

ax5 = figure(5);
hold on
for k = 1:num   %Plot in increasing order of pressure
    j = ind(k);
    if j == 1
        plot(mProp{j},Tt{j},'--','Color',ColorList(k,:))
    else
        plot(mProp{j},Tt{j},'Color',ColorList(k,:))
    end
end
legend(leg,'Interpreter','latex')
xlabel('Propellant Used (kg)','Interpreter','latex')
ylabel('Nitrogen tank temperature ($^{\circ}$C)','Interpreter','latex')
title('Nitrogen Tank Temperature over Propellant Used','Interpreter','latex')
hold off

ax6 = figure(6);
hold on
for k = 1:num   %Plot in increasing order of pressure
    j = ind(k);
    if j == 1
        plot(mProp{j},Pt{j},'--','Color',ColorList(k,:))
    else
        plot(mProp{j},Pt{j},'Color',ColorList(k,:))
    end
end
legend(leg,'Interpreter','latex')
```

```
xlabel('Propellant Used (kg)','Interpreter','latex')
ylabel('Nitrogen tank pressure (psia)','Interpreter','latex')
title('Nitrogen Tank Pressure over Propellant Used','Interpreter','latex')
hold off

ax7 = figure(7);
hold on
for k = 1:num   %Plot in increasing order of pressure
    j = ind(k);
    if j == 1
        plot(mProp{j},HopDist{j},'--','Color',ColorList(k,:))
    else
        plot(mProp{j},HopDist{j},'Color',ColorList(k,:))
    end
end
legend(leg,'Location','northwest','Interpreter','latex')
xlabel('Propellant Used (kg)','Interpreter','latex')
ylabel('Hop Distance (km)','Interpreter','latex')
title('Hop Distance over Propellant Used','Interpreter','latex')
hold off

ax8 = figure(8);
hold on
DistX = zeros(num,1);   %Initialize additional arrays
DistY = DistX;
ResidY = DistX;
for k = 1:num   %Fill arrays
    j = ind(k);
    DistY(k) = max(HopDist{j});
    ResidY(k) = mN2List(j) - max(mProp{j});
    DistX(k) = PressList(j);
end
plot(DistX,DistY)
% leg2 = '
% legend(leg2,'Location','northwest','Interpreter','latex')
xlabel('Tank Pressure (psia)','Interpreter','latex')
ylabel('Maximum Hop Distance (km)','Interpreter','latex')
title('Maximum Hop Distance over Initial Tank Pressure','Interpreter','latex')
hold off

ax9 = figure(9);
hold on
plot(DistX,ResidY)
xlabel('Tank Pressure (psia)','Interpreter','latex')
ylabel('Tank Residuals (kg)','Interpreter','latex')
title('Residual Propellant in Tank over Initial Tank Pressure','Interpreter','latex')
hold off

print(ax1, 'FvarP','-dpng') %Print plots to pngs
print(ax2, 'IspvarP','-dpng')
print(ax3, 'IvarP','-dpng')
print(ax4, 'TSvarP','-dpng')
print(ax5, 'TTvarP','-dpng')
print(ax6, 'PTvarP','-dpng')
print(ax7, 'HDvarP','-dpng')
print(ax8, 'MHDvarP','-dpng')
print(ax9, 'TRvarP','-dpng')
```

Listing 2 Code for determining lithium heating time

```
clc; close all; clear all;

mBlock = 25;    %Mass of lithium block
Pow = 500;  %Available thermal power for melting
MW = 6.941; %Molecular weight of lithium
DHf = 2380; %Heat of formation

Tstart = 548;   %Starting temperature
Tfinal = 1200;  %Final temperature
%%
As = 169.552;   %NIST coefficients for solid lithium Cp
Bs = -882.711;
Cs = 1977.438;
Ds = -1487.312;
Es = -1.609635;

Al1 = 32.46972; %NIST coefficients for low temp liquid lithium Cp
Bl1 = -2.635975;
Cl1 = -6.327128;
Dl1 = 4.230359;
El1 = 0.005686;

Al2 = 26.00896; %NIST coefficients for high temp liquid lithium Cp
Bl2 = 5.632375;
Cl2 = -4.013227;
Dl2 = 0.873686;
El2 = 0.344150;

if Tfinal<Tstart    %Flip order if cooling
    temp = Tfinal;
    Tfinal = Tstart;
    Tstart = temp;
end

if Tstart<0 %Sort by starting temperatures
    disp('Start below range')
elseif Tstart<180.5
    if Tfinal<180.5 %Sort by end temperatures
        T = (Tstart+273.15):0.1:(Tfinal+273.15);    %Array of temperatures, [K]
        Leak = 0.000000000132*T.^4 - 0.000000151512*T.^3 + 0.000114429694*T.^2 - 0.015905719856*T +
            3.862577699137;  %Thermal block heat leak at given temperatures, [W]
        Cp = As + Bs*T/1000 + Cs*(T/1000).^2 + Ds*(T/1000).^3 + Es./(T/1000).^2;    %Cp array at given
             temperatures, [J/mol*K]
        KpS = Cp/MW*1000*mBlock./(Pow-Leak);    %Calculate heating rate, [s/K]
        time = trapz(T,KpS);    %Integrate total heating time, [s]
    elseif Tfinal<426.85
        T = (Tstart+273.15):0.1:(180.5+273.15); %Array of temperatures, [K]
        Leak = 0.000000000132*T.^4 - 0.000000151512*T.^3 + 0.000114429694*T.^2 - 0.015905719856*T +
            3.862577699137;  %Thermal block heat leak at given temperatures, [W]
        Cp = As + Bs*T/1000 + Cs*(T/1000).^2 + Ds*(T/1000).^3 + Es./(T/1000).^2;    %Cp array at given
             temperatures, [J/mol*K]
        KpS = Cp/MW*1000*mBlock./(Pow-Leak);    %Calculate heating rate, [s/K]
        time = trapz(T,KpS);    %Integrate total heating time, [s]

        Hf = DHf/MW*1000;   %Heat of formation, [J/kg*K]
        T = 180.5+273.15;   %Temperature, [K]
        Leak = 0.000000000132*T.^4 - 0.000000151512*T.^3 + 0.000114429694*T.^2 - 0.015905719856*T +
```

```
            3.862577699137;  %Heat leak at given temperature, [W]
        time = time + Hf/(Pow-Leak);    %Time to heat through melting point, [s]

        T = (180.5+273.15):0.1:(Tfinal+273.15); %Array of temperatures, [K]
        Leak = 0.000000000132*T.^4 - 0.000000151512*T.^3 + 0.000114429694*T.^2 - 0.015905719856*T +
            3.862577699137;  %Thermal block heat leak at given temperatures, [W]
        Cp = Al1 + Bl1*T/1000 + Cl1*(T/1000).^2 + Dl1*(T/1000).^3 + El1./(T/1000).^2;   %Cp array at
            given temperatures, [J/mol*K]
        KpS = Cp/MW*1000*mBlock./(Pow-Leak);    %Calculate heating rate, [s/K]
        time = time + trapz(T,KpS); %Integrate total heating time, [s]
    elseif Tfinal<1620
        T = (Tstart+273.15):0.1:(180.5+273.15);
        Leak = 0.000000000132*T.^4 - 0.000000151512*T.^3 + 0.000114429694*T.^2 - 0.015905719856*T +
            3.862577699137;  %Thermal block heat leak at given temperatures, [W]
        Cp = As + Bs*T/1000 + Cs*(T/1000).^2 + Ds*(T/1000).^3 + Es./(T/1000).^2;    %Cp array at given
             temperatures, [J/mol*K]
        KpS = Cp/MW*1000*mBlock./(Pow-Leak);     %Calculate heating rate, [s/K]
        time = trapz(T,KpS);    %Integrate total heating time, [s]

        Hf = DHf/MW*1000;   %Heat of formation, [J/kg*K]
        T = 180.5+273.15;   %Temperature [K]
        Leak = 0.000000000132*T.^4 - 0.000000151512*T.^3 + 0.000114429694*T.^2 - 0.015905719856*T +
            3.862577699137;  %Thermal block heat leak at given temperature, [W]
        time = time + Hf/(Pow-Leak);    %Time to heat through melting point, [s]

        T = (180.5+273.15):0.1:(426.85+273.15); %Array of temperatures, [K]
        Leak = 0.000000000132*T.^4 - 0.000000151512*T.^3 + 0.000114429694*T.^2 - 0.015905719856*T +
            3.862577699137;  %Thermal block heat leak at given temperatures, [W]
        Cp = Al1 + Bl1*T/1000 + Cl1*(T/1000).^2 + Dl1*(T/1000).^3 + El1./(T/1000).^2;   %Cp array at
            given temperatures, [J/mol*K]
        KpS = Cp/MW*1000*mBlock./(Pow-Leak);     %Calculate heating rate, [s/K]
        time = time + trapz(T,KpS); %Integrate total heating time, [s]

        T = (426.85+273.15):0.1:(Tfinal+273.15);    %Array of temperatures, [K]
        Leak = 0.000000000132*T.^4 - 0.000000151512*T.^3 + 0.000114429694*T.^2 - 0.015905719856*T +
            3.862577699137;  %Thermal block heat leak at given temperatures, [W]
        Cp = Al2 + Bl2*T/1000 + Cl2*(T/1000).^2 + Dl2*(T/1000).^3 + El2./(T/1000).^2;   %Cp array at
            given temperatures, [J/mol*K]
        KpS = Cp/MW*1000*mBlock./(Pow-Leak);     %Calculate heating rate, [s/K]
        time = time + trapz(T,KpS); %Integrate total heating time, [s]
    else
        disp('Final above range')
    end
elseif Tstart<426.85
    if Tfinal<426.85
        T = (Tstart+273.15):0.1:(Tfinal+273.15);    %Array of temperatures, [K]
        Leak = 0.000000000132*T.^4 - 0.000000151512*T.^3 + 0.000114429694*T.^2 - 0.015905719856*T +
            3.862577699137;  %Thermal block heat leak at given temperatures, [W]
        Cp = Al1 + Bl1*T/1000 + Cl1*(T/1000).^2 + Dl1*(T/1000).^3 + El1./(T/1000).^2;   %Cp array at
            given temperatures, [J/mol*K]
        KpS = Cp/MW*1000*mBlock./(Pow-Leak);    %Calculate heating rate, [s/K]
        time = trapz(T,KpS);    %Integrate total heating time, [s]
    elseif Tfinal<1620
        T = (Tstart+273.15):0.1:(426.85+273.15);    %Array of temperatures, [K]
        Leak = 0.000000000132*T.^4 - 0.000000151512*T.^3 + 0.000114429694*T.^2 - 0.015905719856*T +
            3.862577699137;  %Thermal block heat leak at given temperatures, [W]
        Cp = Al1 + Bl1*T/1000 + Cl1*(T/1000).^2 + Dl1*(T/1000).^3 + El1./(T/1000).^2;   %Cp array at
            given temperatures, [J/mol*K]
        KpS = Cp/MW*1000*mBlock./(Pow-Leak);    %Calculate heating rate, [s/K]
```

```
        time = trapz(T,KpS);    %Integrate total heating time, [s]

        T = (426.85+273.15):0.1:(Tfinal+273.15);    %Array of temperatures, [K]
        Leak = 0.000000000132*T.^4 - 0.000000151512*T.^3 + 0.000114429694*T.^2 - 0.015905719856*T +
            3.862577699137;  %Thermal block heat leak at given temperatures, [W]
        Cp = Al2 + Bl2*T/1000 + Cl2*(T/1000).^2 + Dl2*(T/1000).^3 + El2./(T/1000).^2;   %Cp array at
            given temperatures, [J/mol*K]
        KpS = Cp/MW*1000*mBlock./(Pow-Leak);    %Calculate heating rate, [s/K]
        time = time + trapz(T,KpS); %Integrate total heating time, [s]
    else
        disp('Final above range')
    end
elseif Tstart<1620
    if Tfinal<1620
        T = (Tstart+273.15):0.1:(Tfinal+273.15);    %Array of temperatures, [K]
        Leak = 0.000000000132*T.^4 - 0.000000151512*T.^3 + 0.000114429694*T.^2 - 0.015905719856*T +
            3.862577699137;  %Thermal block heat leak at given temperatures, [W]
        Cp = Al2 + Bl2*T/1000 + Cl2*(T/1000).^2 + Dl2*(T/1000).^3 + El2./(T/1000).^2;   %Cp array at
            given temperatures, [J/mol*K]
        KpS = Cp/MW*1000*mBlock./(Pow-Leak);    %Calculate heating rate, [s/K]
        time = trapz(T,KpS);    %Integrate total heating time, [s]
    else
        disp('Final above range')
    end
else
    disp('Start above range')
end

time = time/3600    %Convert heating time to hours
```


Acknowledgments

The Triton Hopper design study was supported by the NASA Innovative Advanced Concepts project at NASA Headquarters.

Miles McKaig and Thomas O'Brien would like to thank Dr. Geoffrey A. Landis for his support and guidance through our internship, which was critical to the successful completion of this project. We'd also like to thank the COMPASS team for their assistance with this project.

References

[1] Machado-Rodriguez, J. P., and Landis, G. A., "Analysis of a Radioisotope Thermal Rocket Engine," *AIAA Science and Technology Forum & Exposition 2017*, Grapevine TX, 2017.

[2] *Final Environmental Impact Statement for the Cassini Mission*, National Aeronautics and Space Administration, June 1995. Chapter 2, pages 2-14 and 2-52.

[3] *Final Environmental Impact Statement for the New Horizons Mission*, National Aeronautics and Space Administration, Jly 2005. Volume 1, Chapter 2, page 2-19.

[4] Kaufman, W. B., and Tower, L. K., "Compatability of Sodium and Lithium in Superalloy Heat Pipes," Tech. rep., AF Wright Aeronautical Laboratories, 1985.

[5] Chen, C.-H., and Pearlman, H., "Syngas Production by Thermochemical Conversion of H_2O and CO_2 Mixtures Using a Novel Reactor Design," Tech. rep., Advanced Cooling Technologies, 2013.

[6] Lundberg, L. B., "A Critical Evaluation of Molybdenum and Its Alloys for Use in Space Reactor Core Heat Pipes," Tech. rep., Los Alamos National Laboratory, 1981.

[7] Silverstein, C. C., "Heat Pipe Cooling for Scramjet Engines," Tech. rep., NASA, 1988.

[8] Geoffrey A. Landis, S. R. O., and the NASA Glenn COMPASS team, "Design Study of a Rocket powered Hopper Mission to Triton," *AIAA Space 2017 Forum*, Orlando, FL, 2017.